

# ECCV Caption: Correcting False Negatives by Collecting Machine-and-Human-verified Image-Caption Associations for MS-COCO

Sanghyuk Chun Wonjae Kim Song Park Minsuk Chang Seong Joon Oh

NAVER AI Lab

## Abstract

Image-Text matching (ITM) is a common task for evaluating the quality of Vision and Language (VL) models. However, existing ITM benchmarks have a significant limitation. They have many missing correspondences, originating from the data construction process itself. For example, a caption is only matched with one image although the caption can be matched with other similar images, and vice versa. To correct the massive false negatives, we construct the Extended COCO Validation (ECCV) Caption dataset by supplying the missing associations with machine and human annotators. We employ five state-of-the-art ITM models with diverse properties for our annotation process. Our dataset provides  $\times 3.6$  positive image-to-caption associations and  $\times 8.5$  caption-to-image associations compared to the original MS-COCO. We also propose to use an informative ranking-based metric, rather than the popular Recall@K(R@K). We re-evaluate the existing 25 VL models on existing and proposed benchmarks. Our findings are that the existing benchmarks, such as COCO 1K R@K, COCO 5K R@K, CxC R@1 are highly correlated with each other, while the rankings change when we shift to the ECCV mAP. Lastly, we delve into the effect of the bias introduced by the choice of machine annotator. Source code and dataset are available at <https://github.com/naver-ai/eccv-caption>

## 1 Introduction

Image-caption aligned datasets (*e.g.*, MS-COCO Caption [1, 2], Conceptual Caption [3, 4], RedCaps [5]) have become *de-facto* standard datasets for training and evaluating Vision-Language (VL) models. Particularly, Image-to-Text Matching (ITM) tasks [6–23] are widely used benchmark for evaluating a VL model. The existing ITM benchmark datasets are built by annotating captions (by alt-texts [3, 4, 24], web crawling [5], or human annotators [2]) for each image without considering possible associations with other images in the dataset. During training and evaluation, the collected image-caption pairs are treated as the only positives in the dataset, while other pairs are considered the negatives. However, in practice, there exists more than one caption to describe one image. For example, the description “The man is playing tennis with a racket”, chosen from the MS-COCO Caption dataset, may describe multiple images with tennis players equally well (Figure 1). We have observed that the number of missing positives is tremendous; there exist  $\times 3.6$  positive image-to-caption correspondences and  $\times 8.5$  caption-to-image correspondences than the original MS-COCO dataset.

While the huge number of false positives in VL datasets is potentially sub-optimal for training VL models, it is downright detrimental for evaluation. For example, the small number of positive correspondences of image-caption aligned datasets<sup>1</sup> limits the evaluation metrics. In other tasks, such as the image retrieval with CUB [25], CARS [26], SOP [27], and InShop [28] benchmarks, the positives and negatives are defined by

<sup>1</sup>In MS-COCO Caption, a caption is only matched to one image and an image is matched to five captions. Other datasets usually have one caption for each image.



The man is playing tennis with a racket  
A man taking a swing at a tennis ball  
A man on a court swinging a tennis racket  
A tennis player swinging a racket at a ball  
A person hitting a tennis ball with a tennis racket  
The man is playing tennis on the court  
A man with a tennis racket swings at a tennis ball



Figure 1: **Inherent multiplicity of correspondences in MS-COCO Caption.** While any image-caption pair above makes sense (positive pair), only red and blue image-caption pairs are marked as positive in MS-COCO Caption.

the pre-defined classes; hence, the number of possible matched items are large enough to measure precision or mean average precision (mAP) metrics. On the other hand, because the existing ITM benchmarks only have one positive correspondence for each item, they are only able to use recall-based metrics (e.g., Recall@ $k$ ) that are known to be less informative than the precision- or ranking-based evaluation metrics [29]. In this paper, we focus on correcting the false negatives in the evaluation dataset and the recall-based evaluation metrics to make a fair comparison of VL models.

As our first contribution, we correct the false negatives in the original MS-COCO Caption dataset by constructing an extended version of MS-COCO dataset, named Extended COCO Validation (ECCV) Caption dataset. We annotate whether each image-caption pair in MS-COCO Caption is positive with the crowdsourced human workers. The labor cost for this process scales quadratically with the size of the dataset (e.g., MS-COCO Caption has 76B possible image-caption pairs, while the number of images is only 123K). Since verifying every possible image-text pair is not scalable, we subsample the queries in the dataset and reduce the number of candidates for positive matches with the machine-in-the-loop (MITL) annotation process. MITL lets a model reduce the number of candidate positives; human annotators then evaluate the machine-selected candidates. We employ five state-of-the-art ITM models with distinct properties as the machine annotators; CLIP [24], ViLT [30], VSRN [13], PVSE [14], and PCME [20]. After a post-processing, ECCV Caption contains 1,261 image queries (originally 5,000) but with 17.9 positive captions per image query on average (originally 5). It also contains 1,332 caption queries (originally 25,000) with 8.5 positive images per caption (originally 1).

While the use of machine annotator is inevitable for the sake of scalability, the choice of a particular machine annotator may bias the dataset towards the specifics of the model. This can be problematic because different models show different filtered results to the human annotators, that brings the impartialness of the annotated dataset towards any particular model to the surface. In other words, the MITL annotations are not stable across model choices. Our studies show that the underlying ML model conditions the annotated dataset towards favoring certain models over the others. This practice will thus potentially lead to the danger of biased evaluation results using such datasets. We show that the rankings among the ITM models can be arbitrarily shifted by modifying the underlying ML model. Our study also shows that using more machine annotators can alleviate the machine bias in the dataset construction. We remark that the findings are applicable to a wide range of tasks where users put labels on samples from a long list of candidate classes; our task is a special case of such a framework.

A similar MITL approach to ECCV Caption for expanding the positive matches was also employed by Parekh *et al.* [31], resulting in the dataset CrissCrossed Caption (CxC). However, CxC focus on scoring the text-to-text similarities, resulting in many missing positives in the text-to-image relationship. Furthermore, CxC only employs one language-based machine annotator, that can lead a biased dataset as our observation. Our ECCV Caption focuses on the inter-modality relationship and utilizes five ITM methods to avoid the biased dataset construction. As another attempt to correct COCO benchmark, Chun *et al.* [20] annotate pseudo-positives by using the COCO instance classes, called Plausible Match (PM). For example, both images in Figure 1 contain the same object class, “tennis racket”. Hence, the red and blue captions are considered positives for both red and blue images. Although PM items can detect most of the false negatives, it also introduces many false positives. Compared to PM [20] which rely on noisy proxies for correspondence, we correct the missing false negatives with “human ground truths” with the help of machine annotations. All in all, our dataset results in a higher recall than CxC and high precision than PM.

Now that the false negatives are corrected in the evaluation sets, we re-examine the known ranking of the state-of-the-art VL models evaluated in the existing benchmarks. Our second contribution is the re-evaluation of 25 state-of-the-art VL models on ITM tasks with nine different metrics. With the presence of

multiple evaluation metrics, we have been able to group them according to the preservation of rankings of VL models. We have observed that COCO 5K R@1 & R@5 and CxC R@1 are highly correlated (larger than 0.87 Kendall’s rank correlation  $\tau$ ). On the other hand, we observe that the rankings across methods measured by mAP@R on ECCV Caption and COCO 1K R@1 are less well-correlated ( $\tau = 0.47$ ). This confirms the observation by Musgrave *et al.* [29] and Chun *et al.* [20] on class-based datasets. We argue that R@1 can overestimate the model performance by focusing only on the accuracy of the top-1 retrieved item rather than the rest of the items. We show examples where the rankings change dramatically according to the evaluation metric.

Our contributions are as follows. (1) We construct Extended COCO Validation (ECCV) Caption dataset to correct a large number of false negatives in the COCO Caption test split. (2) We re-evaluate 25 state-of-the-art VL models on our ECCV Caption dataset based on a ranking-based metric (mAP@R) instead of Recall@ $k$ . We show that the rankings between R@1 and mAP@R are rarely preserved. (3) We explore the effect of the choice of the machine annotators to ECCV Caption. Our analysis shows that using more model will alleviate the potential biases of the annotated dataset.

## 2 Related Works

### 2.1 Noisy many-to-many correspondences of image-caption datasets

There have been a few attempts to introduce many-to-many or noisy correspondences for VL datasets. Parekh *et al.* [31] construct CrissCrossed Caption (CxC) dataset by employing a similar MITL approach to ours. However, CxC focuses on intra-modality similarity, particularly the text-to-text. They employed the Universal Sentence Encoder [32] and average bag-of-words (BoW) based on GloVe embeddings [33], while we directly focus on the inter-modality relationships and utilizes powerful state-of-the-art ITM methods (*e.g.*, CLIP [24], ViLT [30], VSRN [13], PVSE [14], and PCME [20]) to select candidates for validation by humans. CxC contains human ratings for 89,555 image-to-caption associations, among which 35,585 are positive,  $\times 1.4$  more positive relationships than 25,000 in the COCO Captions. We show that the additional positives by CxC are precise, but their annotations still have many missing positives (*i.e.*, high precision but low recall), resulting that R@1 on CxC perfectly preserves the rankings of VL models on COCO 5K R@1. On the other hand, our ECCV Caption has  $\times 4.4$  positives ( $\times 3.6$  image-to-caption correspondences and  $\times 8.5$  caption-to-image correspondences) compared to COCO Captions and roughly three times more positives compared to CxC. Furthermore, it is possible to measure mAP on our dataset due to the abundance of positive pairs, unlike for CxC.

Another attempt by Chun *et al.* [20] focused on the precision rather than R@1 by annotating the pseudo-positives in a fully algorithmic approach. The authors defined “plausible matching (PM)” items that have same instance classes with the query image (or the image corresponding to the query caption) to annotate pseudo-positives. For example, both images in Figure 1 contain the same instance class, “tennis racket”, leading to the conclusion that the red and blue captions are marked as positives for both red and blue images. More precisely, two instances are PM if  $y_1, y_2 \in \{0, 1\}^d$  differ at most  $\zeta$  positions, where  $d$  is the number of instance classes in the dataset (*e.g.*, for COCO,  $d = 80$ ). PM Using the class-based pseudo-positives, Chun *et al.* propose the Plausible-Match R-Precision (PMRP) metric, an R-Precision [29] metric based on the “Plausible-Match” (PM) policy. The authors propose to use multiple  $\zeta$  (*e.g.*,  $\zeta \in \{0, 1, 2\}$ ) and report the average precision value. PM items can detect many missing false positives in the dataset, but we observe that the most of PM pseudo-positives are not actual positives (*i.e.*, high recall but low precision) — See Table 2. We also observe that PMRP shows a low correlation to other evaluation metrics; PMRP is a noisy metric compared to others.

### 2.2 Machine-in-the-loop (MITL) annotation

Humans and machines complement each other in the annotation process as they have different comparative advantages. Humans are the ultimate source of true labels, but they are slow and prone to errors and biases [34–36]. Machines are highly scalable, but their generalizability to unseen samples is limited. Machines are also prone to their own versions of errors and biases [37, 38]. The machine-in-the-loop (MITL) annotations have been designed to take the best of both worlds [39–42]. We group and explain MITL methods in detail.

Depending on the required trade-off between annotation quality and efficiency, one may opt for either single-turn or multi-turn annotation pipeline. The latter serves for the maximal demand for annotation quality: humans and machines alternate to correct and learn from each other’s annotations [40, 42]. This is

Model	Text backbone	Visual backbone	Objective function
PVSE [14]	Bi-GRU [57]	ResNet-152 [51]	Multiple instance learning
VSRN [13]	Bi-GRU	Faster R-CNN [59]	Semantic reasoning matching
PCME [20]	Bi-GRU	ResNet-152	Probabilistic matching
ViLT [30]	Transformer [58, 60]	Transformer	Vision-language pretraining
CLIP [24]	Transformer	Transformer	Contrastive learning

Table 1: **Overview of the employed machine annotators.** Differences among five state-of-the-art cross-modal retrieval models in terms of architectures and training objectives are shown. ViLT and CLIP are trained on a massive amount of aligned vision-language data, while other methods only use MS-COCO Caption.

widely used technique, the applications ranging from building a dictionary of cooking vocabularies [43], to supporting real-time real-world screen-reading for blind people [44] and characterizing system failures [45]. In this work, we focus on the *single-turn MITL annotations* to focus on the atomic building block for MITL pipelines in general. There are two types for the single-turn paradigm: machine-verified human annotations or human-verified machine annotations. While there exists a field of research on the former [46, 47], we focus on the latter, which are highly relevant for dealing with huge sources of data.

Under the human-verification framework, machines make label proposals for each image, focusing more on the recall than precision [48, 49]. For example, OpenImages dataset [49], which contains 19,794 candidate labels, is labeled by first generating label proposals by high-performance image classifiers like Inception [50] and ResNet [51] architectures. Previous crowdsourcing research in human-computer interaction (HCI) had mainly focused on the annotation interface and their effects on the annotation [52–54], or building crowdsourcing workflow that leverage microtask pipelines [55, 56]. This paper investigates the side effects of the model choice in the MITL annotation paradigm with human-verified machine annotations where machines provide candidate label proposals.

### 3 ECCV Caption Dataset Construction

In this section, we describe ECCV Caption construction details. We annotate image-caption pairs in MS-COCO to solve the multiplicity of MS-COCO. However, the number of candidates is too huge for an exhaustive verification by humans: 76B for the whole dataset, and 125M for the test split only. To reduce the amount of judgements by humans, we employ a single-turn machine-in-the-loop (MITL) annotation pipeline, containing three stages: (1) Filtering by machine annotators. (2) Judging the filtered relationships by MTurkers and additional verification by internal workers. (3) Post-processing and merging with CxC.

#### 3.1 Model candidates for machine annotators

We choose five ITM models with diverse properties to cover both diversity and practical relevance. The models use different text backbones (Bi-GRU [57], Transformer [58]), visual backbones (ResNet-152 [51], Faster R-CNN [59], ViT [60]), training objective functions, and training datasets as shown in Table 1. We use the official released pre-trained weights by the authors except PCME. Because PCME shows worse retrieval performances than others, we re-train PCME by using CutMix [61] pretrained ResNet-152 [51] to match the retrieval performances with others. We employ CLIP ViT-B/32 model as a machine annotator. We describe more details of each method in Appendix A.1.

We quantify the diversity of the models by measuring the differences in their retrieved items. We first retrieve top-25 images for each model on the captions of COCO Caption test split. We measure the similarities of the models in two different metrics. First, for every pair of models, we measure the Kendall rank correlation [62] between the two rankings of the retrieved items by the models. We observe that the models usually have low similarity ( $\tau < 0.3$ ), except for PVSE and PCME. We additionally measure, for each pair of model  $i$  and  $j$ , the average ranking of model  $i$ 's top-1 ranked item by model  $j$ . The top-1 items retrieved by the models are usually not included in the top-3 items by the others. Above two analyses show that the chosen models are diverse and the retrieved items do not correlate that much. The full results are shown in Appendix A.2.

Dataset	I2T Prec	I2T Recall	T2I Prec	T2I Recall
Original MS-COCO Caption	47.3	20.0	89.4	12.8
CxC [31]	39.6	22.0	81.4	15.0
Plausible Match [20]	8.3	74.6	10.5	69.0

Table 2: **Precision and recall of the existing benchmarks.** Precision (Prec) and Recall of previous datasets measured by human verified positive pairs are shown. A low Prec means that many positives are actually negatives, and a low Recall means that there exist many missing positives.

Dataset	# positive images	# positive captions
Original MS-COCO Caption	1,332	6,305 ( $=1,261 \times 5$ )
CxC [31]	1,895 ( $\times 1.42$ )	8,906 ( $\times 1.41$ )
Human-verified positives	10,814 ( $\times 8.12$ )	16,990 ( $\times 2.69$ )
ECCV Caption	11,279 ( $\times 8.47$ )	22,550 ( $\times 3.58$ )

Table 3: **The number of positive images and captions for each dataset.** We show the number of positive items for the subset of the COCO Caption test split. The number of query captions and images are 1,332 and 1,261, respectively.

### 3.2 Crowdsourcing on Amazon Mechanical Turk

We crowdsource image-caption matches on Amazon Mechanical Turk (MTurk) platform. For the sake of scalability, we subsample 1,333 caption queries and 1,261 image queries from the COCO Caption test split. Since the number of all possible matches is still prohibitive (40M), we employ the filtering strategy to reduce the number of candidates for human verification. We pre-select top-5 captions and images retrieved by the five models. After we remove the duplicate pairs from the  $(1,261 + 1,333) \times 5 \times 5 = 64,850$  pairs, 46,424 pairs remain.

We package the task for human annotators into a series of Human Intelligence Tasks (HITs). Each HIT contains 18 machine-retrieved pairs, consisting of 1 true positive (TP) golden pair (*i.e.*, an *original positive pair* in the dataset), 1 true negative (TN) golden pair (random pair, not in the top-25 of any model), and 16 pairs to be annotated. The golden examples are used for the qualification process; if a submitted HIT contains wrong answers to the golden examples, we manually verify the HIT. For each image-caption pair candidate, workers can choose an answer among the choices “100% YES”, “Partially YES, but”, “Mostly NO, because”, and “100% NO”. Here, we use four choices instead three level (“YES”, “Not Sure”, and “NO”) to discourage workers from selecting “Not Sure” for all the questions. We have assigned 2,160 HITs, consisting of 43,200 pairs to be verified, to 970 MTurk workers. The crowdsourcing details, including an example HIT, compensation details, and worker statistics are in Appendix B.1 and Appendix B.2.

### 3.3 Postprocessing MTurk annotations

We observe that 21,995 associations among 43,200 associations are annotated as positives (“Yes” or “Weak Yes”) by the workers. The detailed statistics for each machine annotator can be found in Appendix B.3. We then filter out 18 meaningless captions (*e.g.*, “I am unable to see an image above”), 14 wrong captions found by workers (*e.g.*, “A group of birds flying above the beach” for the image with many kites) and 1 duplicate image found in the training set. The full list of the filtered items can be found in Appendix C.1.

Using the 21,995 human verified positives, we report precision and recall of the existing benchmarks. Let  $t_i$  be the set of human-annotated positives for the query  $i$  in Section 3.2 and  $r_i$  be the set of positives for  $i$  in the target dataset. We define precision and recall of a dataset as  $Prec = \frac{1}{N} \sum_{i=1}^N \frac{|r_i \cap t_i|}{|r_i|}$  and  $Recall = \frac{1}{N} \sum_{i=1}^N 1 - \frac{|t_i \setminus r_i|}{|t_i|}$ . Table 2 shows precision and recall of the original COCO Caption, CxC [31], and Plausible Match (PM) pseudo-positives [20]. While the original COCO and CxC show high precisions, we observe that their recall is significantly low, around or less than 20%. Evaluating models on such a low-recall dataset with the R@1 metric can be highly misleading. A model may be able to retrieve good enough positive items which are not captured in the dataset, resulting in erroneously low R@1 scores. On the other hand, more than 70% of the positives can be captured by PM, but only about 10% pseudo-positives are correct.

We consider the CxC positives as the additional sixth machine-human verified annotations, and extend our human verified positives with CxC positives to construct the final ECCV Caption. Table 3 shows the detailed statistics of CxC, human-verified positives, and our ECCV Caption. Overall, ECCV Caption has  $\times 8.47$  positive images and  $\times 3.58$  positive captions than the original dataset. Figure 3a shows the number



Figure 2: **Example positive sample from ECCV Caption.** The given caption query: “A herd of zebras standing together in the field”. **Red:** original positive. **Green:** annotated as “100% Yes”. **Blue:** annotated as “Weak Yes”.

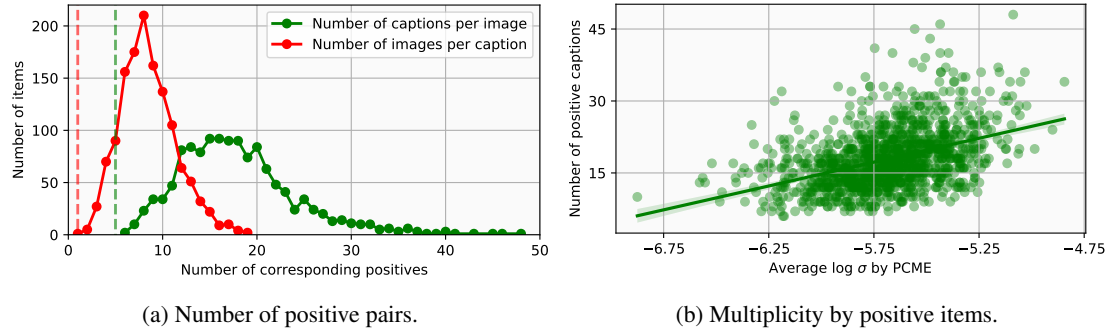


Figure 3: **Multiplicity captured by ECCV Caption.** (a) Number of positive pairs in ECCV Caption is shown. Dashed lines denote the number of the original COCO Caption positives (1 image for each caption, and 5 captions for each image). ECCV Caption contains plenty positive items per each modality. (b) The scatter plot of the PCME-predicted multiplicity against the number of positive captions for each image is shown. There exists a positive correlation.

of positive images and captions per each item; there exist many positives beyond the original COCO associations. We illustrate example image-caption pairs from ECCV Caption in Figure 2 and Appendix C.2.

We additionally analyze the multiplicity of ECCV Caption by PCME [20] that produces an uncertainty score for each query that represents the degree of multiplicity. Figure 3b shows that more uncertain images correspond to more captions in the annotated dataset. In other words, our new annotations capture the hidden false negatives in the original COCO Caption well.

## 4 Re-evaluation of ITM models on ECCV Caption

In this section, we re-evaluate the existing image-to-text matching (ITM) models on our new dataset and previous benchmarks. We first introduce the evaluation metrics (§4.1) and comparison methods (§4.2) for our benchmark. We compare the performances and analyze the results (§4.3).

### 4.1 Evaluation metrics

The existing ITM benchmarks (*e.g.*, COCO Caption) use Recall@ $k$  metrics, particularly Recall@1 (R@1). Specifically, previous works measure R@1 for 5-fold validation splits (*i.e.*, each split has 1K images), and for the full test split [63]. The former is called COCO 1K R@ $k$  and the latter is called COCO 5K R@ $k$ , respectively. Previous studies separately report image-to-text, text-to-image retrieval R@1, R@5 and R@10 scores. However, as shown by Musgrave *et al.* [29], R@ $k$  is not an informative metric; embedding spaces with nearly 100% R@1 can have different properties. The problem becomes even worse for the ITM benchmarks, whose queries only have very few (usually only one) references: Even if a model correctly retrieves plausible items that are not among the set of original positives, the current benchmark cannot evaluate the model correctly. It is common to use larger values of  $k$  to less penalize wrong yet plausible predictions. However, as shown in Figure 3a, the actual number of plausible positives can be larger than typical choice of  $k$  (*e.g.*, 5 or 10). Instead, we suggest to use mAP@ $R$  [29], a modified mAP measured by retrieving  $R$  items where  $R$  is the number of positives for the query. Previous ITM benchmarks cannot employ mAP@ $R$  because  $R$  is too small (*i.e.*, 1). Thanks to our human-verified ground-truth positives, we can reliably measure mAP@ $R$  on ECCV Caption. We also report modified Plausible Match R-Precision (PMRP) scores by changing  $R$  to  $\min(R, 50)$ , because the number of pseudo-positives  $R$  can be very large (*e.g.*, larger than 10,000) but most of them are not actual positive (Table 2). While Chun *et al.* [20] proposed to use the average R-Precision for three different thresholds, (*e.g.*,  $\zeta = \{0, 1, 2\}$ ), we only report PMRP

	ECCV Caption			CxC	COCO		
	mAP@R	R-P	R@1	R@1	1K R@1	5K R@1	PMRP
ResNet-152 [51] image encoder + Bi-GRU [57] text encoder							
VSE0 <sup>†</sup> [9]	22.67	33.27	55.55	24.24	34.14	22.27	46.95
VSE++ <sup>†</sup> [9]	35.01	45.50	73.11	37.95	48.46	35.79	54.26
PVSE K=1 [14]	33.98	44.49	73.25	38.38	48.67	36.20	53.56
PVSE K=2 [14]	<u>40.26</u>	<u>49.92</u>	<u>76.74</u>	<u>40.18</u>	<u>50.29</u>	<u>38.13</u>	55.52
PCME [20]	37.11	47.82	74.79	40.09	<u>50.29</u>	38.03	<u>56.71</u>
PCME (CutMix [61] pre-trained) <sup>†</sup> [20]	<b>41.74</b>	<b>51.45</b>	<b>78.67</b>	<b>41.70</b>	<b>51.35</b>	<b>39.51</b>	<b>57.65</b>
Region features based on Bottom-up Attention [64] and SCAN [11]							
VSRN [13]	<b>42.28</b>	<b>51.84</b>	81.51	48.85	58.33	46.74	55.44
VSRN + AOQ [18]	40.94	50.65	81.53	50.10	59.32	48.14	56.41
CVSE [17]	37.35	47.51	76.70	45.82	55.37	43.80	56.49
SGR [19]	35.80	46.04	78.77	50.60	58.87	48.86	56.91
SAF [19]	35.96	46.19	78.36	49.58	59.09	47.80	<u>57.21</u>
VSE infty (BUTD region) [21]	40.46	49.97	82.52	52.40	61.03	50.38	56.64
VSE infty (BUTD grid) [21]	40.40	50.09	<u>83.01</u>	<u>53.47</u>	<u>62.26</u>	<u>51.60</u>	56.87
VSE infty (WSL grid) [21]	<u>42.41</u>	<u>51.43</u>	<b>86.44</b>	<b>60.79</b>	<b>68.07</b>	<b>59.01</b>	<b>57.65</b>
Large-scale Vision-Language pretraining							
CLIP ViT-B/32 [24]	26.75	36.91	67.08	41.97	49.84	40.28	55.32
CLIP ViT-B/16 [24]	29.25	38.99	71.05	44.26	52.32	42.69	56.58
CLIP ViT-L/14 [24]	27.98	37.80	72.17	48.14	55.38	46.44	<b>57.70</b>
VinVL (zero-shot) [65]	22.18	32.93	55.19	33.74	43.51	32.07	47.26
VinVL [65]	<b>40.81</b>	<b>49.55</b>	<u>87.77</u>	<u>67.76</u>	<b>82.38</b>	<u>66.39</u>	54.72
ViLT (zero-shot) [30]	26.84	36.81	69.00	<u>50.35</u>	58.83	48.63	57.38
ViLT [30]	34.58	44.27	77.81	53.72	61.81	52.18	<u>57.63</u>
BLIP [66]	<u>40.52</u>	<u>48.43</u>	<b>90.99</b>	<b>74.30</b>	<u>78.30</u>	<b>73.11</b>	57.17
Different negative mining (NM) strategies							
PVSE K=1, No NM <sup>†</sup>	33.34	44.44	67.99	32.69	43.28	30.65	<b>56.67</b>
PVSE K=1, Semi-hard NM <sup>†</sup> [67]	<b>36.63</b>	<b>47.36</b>	<b>73.97</b>	38.17	48.49	36.00	55.15
PVSE K=1, Hardest NM <sup>†</sup> [9]	35.76	46.50	73.68	<b>39.02</b>	<b>49.12</b>	<b>36.88</b>	54.37

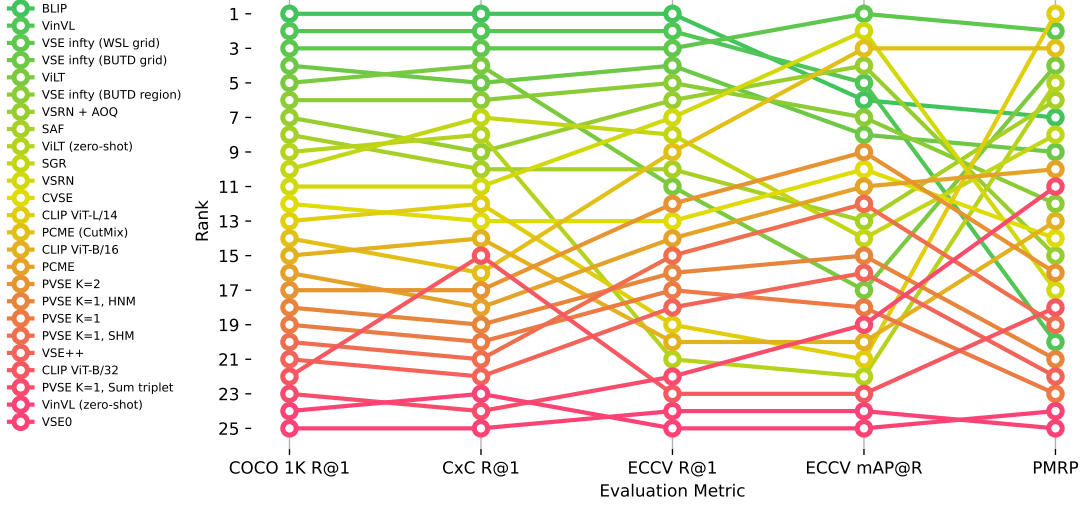
Table 4: **Re-evaluating VL models.** ECCV Caption mAP@R, R-Precision (R-P), Recall@1 (R@1), CxC R@1, COCO 1K R@1, 5K R@1, and PMRP are shown. The numbers are the average between the image-to-text retrieval and text-to-image retrieval results. Full numbers for each modality and COCO R@5 results are in Appendix. <sup>†</sup> denotes our re-implementation and “zero-shot” for VinVL and ViLT denotes VL pre-trained models without fine-tuning on the COCO Caption for the retrieval task.

when  $\zeta = 2$ . We additionally compute R@1, R@5 and PMRP scores on the original COCO Caption, R@1 on CxC, and R@1 and R-Precision on ECCV Caption to analyze correlation between each evaluation metric to ECCV mAP@R.

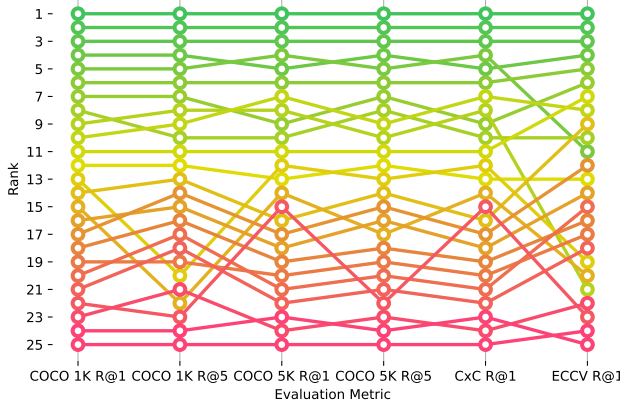
#### 4.2 Evaluated methods

We compare 25 state-of-the-art VL models, whose trained weights are publicly accessible, categorized into four groups: (1) visual semantic embedding (VSE) methods with the ResNet-152 [51] image encoder and Bi-GRU [57] text encoder, including VSE0, VSE++ [9], PVSE [14] (K=1 and K=2), and PCME [20] (the official model and our new implementation); (2) VSE methods with region features extracted by Visual Genome [68] pre-trained Faster R-CNN [59] based on the implementation by Anderson *et al.* [64] and Lee *et al.* [11], including VSRN [13], VSRN + AOQ [18], CVSE [17], SGR, SAF [19], and VSE $\infty$  with BUTD region, grid and WSL grid features [21]<sup>2</sup>. (3) Large-scale vision-language pretraining (VLP) methods, including pre-trained CLIP with ViT-B/32, ViT-B/16 and ViT/L14 backbones [24], pre-trained and fine-

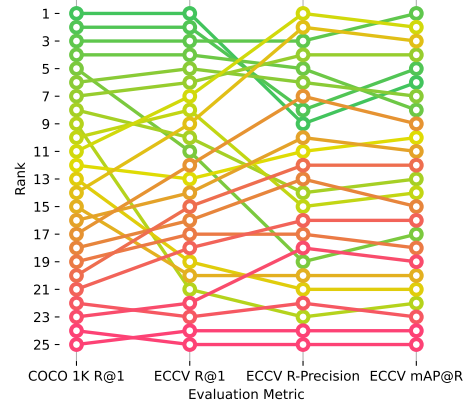
<sup>2</sup>Technically speaking, VSE $\infty$  (WSL grid) does not use region features, but CNN features extracted from Instagram-trained ResNext [69]. This study treats all VSE $\infty$  variants as region feature-based models for convenience.



(a) Comparison of COCO, CxC, ECCV and PMRP.



(b) Comparison of Recall@1 metrics.



(c) Comparison of ECCV metrics.

Figure 4: **Ranking correlation between different evaluation metrics.** Ranking of methods is largely preserved between COCO and CxC Recall@1, while it is rarely preserved among COCO Recall@1, ECCV mAP@R and PMRP.

tuned ViLT [30], pre-trained and fine-tuned VinVL [65], and fine-tuned BLIP [66]. Here, “pre-trained” signifies that the model is trained with a massive image-text aligned dataset, but is not specifically trained for COCO Caption; “fine-tuned” signifies that the VLP model is fine-tuned on COCO Caption for the ITM task. We note that vision-language transformers except CLIP need  $O(|C| \times |I|)$  forward operations to compute the full pairwise ranks between  $|C|$  number of captions and  $|I|$  number of images, while other methods only need  $O(|I|) + O(|C|)$  forward operations to compute the full pairwise ranks based on the cosine similarity. For example, VinVL takes 25 hours to compute the full pairwise ranks for the COCO Caption test split by a single A100 GPU core, while VSE++ only takes 1 minute in the same environment. (4) PVSE models with different negative mining (NM) methods, including no NM, semi-hard NM (SHM) [67], and hardest NM (HNM) [9].

We use the official trained weights for each model with a few exceptions. We re-implement VSE0, VSE++, PCME with CutMix pre-trained ResNet, and PVSE models with various NM strategies. We follow the optimization details in Chun *et al.* [20], such as two-stage optimization, cosine annealing scheduler, and AdamP optimizer [70]. The training details are in Appendix D.1.

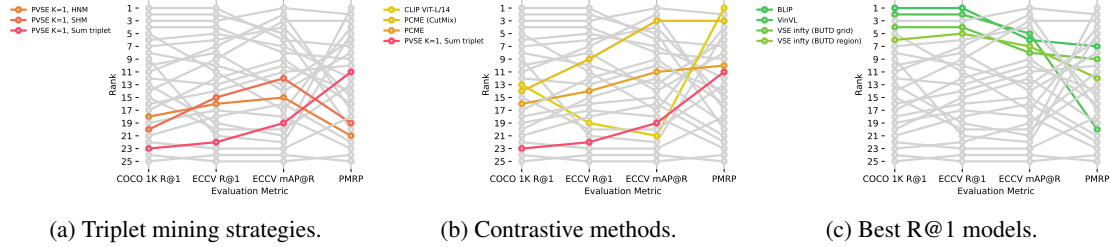


Figure 5: **Rankings of different VL models.** Ranking of (a) PVSE models with diverse triplet mining strategies (b) contrastive methods (c) the best models are shown.

### 4.3 Re-evaluation of ITM methods

Table 4 and Figure 4 shows the full comparisons of 25 VL models with different evaluation metrics. We report the full table including modality-wise results, R@5 scores in Appendix D.2. We first observe that R@ $k$  scores across different datasets have high correlations among themselves (Figure 4b). In terms of the ranking correlation, we observe that COCO 1K R@1 shows almost 0.9 kendall’s rank correlation with the ranking yielded by R@5 (0.87), COCO 5K R@1 (0.89) and R@5 (0.97), or CxC R@1 (0.89). This implies that measuring R@1 or R@5 on different benchmarks, such as the original COCO Caption, CxC, and ECCV Caption are not informative than only measuring Recall@ $k$  on COCO 1K or 5K. On the other hand, the rankings by COCO 1K are not preserved well to PMRP (0.45), ECCV R@1 (0.72), ECCV R-Precision (0.39) and ECCV mAP@ $R$  (0.47) in Kendall’s  $\tau$ . We also observe that the rankings by PMRP are relatively less correlated to the other metrics, such as COCO R@1 (0.45), ECCV R@1 (0.29) or ECCV mAP@ $R$  (0.20) in Kendall’s  $\tau$ . The full Kendall’s  $\tau$  between pairs of evaluation metrics are in Appendix D.3.

Our re-evaluation shows that existing ITM evaluation benchmarks can overestimate the VL model performance by focusing only on COCO R@1, where the rankings between COCO R@1 and ECCV mAP@ $R$  are not largely preserved. For example, we observe that the hardest negative mining technique, previously deemed useful for image-text retrieval tasks, are actually selectively effective for the R@1 metric, rather than for the actual task itself. Under our new metrics like ECCV R@1 and ECCV mAP@ $R$ , we observe that the milder strategy of semi-hard negative mining to be more effective – See Figure 5a. Chun *et al.* [20] also observed a similar pattern in the CUB Caption dataset [25] by using the class-defined positives. Our finding is the first observation in the practical large-scale VL dataset. Similarly, we observe that many large-scale VL pre-training methods with high R@1 scores show inferior ECCV mAP@ $R$  scores compared to other visual semantic embedding techniques. For example, CLIP ViT-L/14 shows superior COCO 1K R@1 than PCME (55.4% and 40.1%, respectively). However, in terms of ECCV mAP@ $R$ , CLIP shows inferior performances than PCME (28.0% and 37.1%, respectively).

Similarly, we observe that PMRP shows different behaviors compared to other metrics. Especially, we observe that the contrastive models without a negative mining strategy are specialized to PMRP metric – Figure 5b. We presume that it is because the contrastive learning strategy enforces the features with the similar objects to be mapped to the similar embedding space. In contrastive the best models on COCO and ECCV (*e.g.*, BLIP, VinVL, and VSE $\infty$ ) show inferior PMRP scores – Figure 5c. We presume that it is because PMRP only captures the existence or absence of the objects, while an optimal retrieval also should consider the plausibility between matched image-caption pairs.

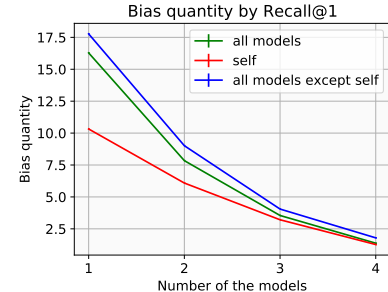
## 5 Choice of Machine Annotators and Dataset Quality

Our dataset construction process contains MITL annotation process, where the choice of the machine annotators can potentially harm the dataset quality. The positives in our dataset are the retrieved items by the machine annotators. If the machines are biased towards undesired patterns (*e.g.* favoring certain items over the others), future methods built on our benchmark will overfit to those patterns. We employ five diverse machine annotators to reduce the potential biases by models. In this section, We explore and quantify the effect of the choice of multiple machine annotators to the dataset quality.

We delve into the effect of the choice of machine annotators used for machine-in-the-loop (MITL) labeling paradigm to the dataset quality. Specifically, we are interested in the model bias, the type of bias that arises because of the pre-selection of plausible samples by the model in the annotation pipeline. We discuss the

Models	Models used for annotations					
	PVSE	VSRN	PCME	ViLT	CLIP	All
PVSE	<b>76.5</b>	63.6	67.6	45.3	42.0	76.6
VSRN	68.0	<b>80.1</b>	69.0	51.1	47.2	<b>80.1</b>
PCME	67.7	64.3	<b>77.3</b>	46.0	44.1	77.4
ViLT	59.5	59.8	58.8	<b>62.0</b>	<b>49.3</b>	72.4
CLIP	51.7	51.5	52.6	42.8	<b>49.3</b>	64.3

(a) Model performances on benchmarks built with different machine annotators.



(b) Number of machine annotators vs. bias quantification.

Figure 6: **Bias quantification in the dataset.** (a) We measure the performances of five models for the caption-to-image retrieval task. We report R@1 metrics measured by different versions of ECCV Caption with different machine annotators. Each column header denotes the machine annotator that proposes positive samples to be annotated by human annotators. “All” denotes the strategy where all five machine annotators are used. (b) The bias quantification with the varying number of models for MITL. We observe that using more models reduce the severity of bias; the discrepancy between the resulting annotations by models and the underlying labels for the samples decreases.

generalizability of our framework to general annotation tasks in Appendix E.1, and the definition of “bias” in our dataset process in Appendix E.2. We measure the model bias by employing the crowdsourced data as the source for evaluating the ITM models. For a perfectly unbiased data, we shall expect the identical rankings across the version of datasets collected with different models.

Table 6a shows the performances on different versions of the datasets using only one MITL model (the detail of dataset construction and full results are in Appendix E.3). Not surprisingly, we observe that the best-performing model for each dataset coincides with the model used for the MITL label proposal (*i.e.*, the diagonal elements in Table 6a). Other models tend to show quite some drop in performance. This strongly corroborates the existence of model bias in datasets collected with the aid of machine filtering. We further observe that even for models not used for generating the label proposals (*i.e.*, the non-diagonal elements in Table 6a), the rankings shift with respect to the underlying MITL model. This suggests that even when one avoids the direct use of the MITL model for evaluating its own performance, one may still observe unstable evaluation results, where different MITL models arbitrarily favor different models.

We additionally measure the distance between a version of dataset and the all-model dataset, which is deemed to contain the labels that are closer to the true labels. We define  $s_{\Theta}(\phi)$  as the performance of the model  $\phi$  evaluated upon the dataset built with the multi-model strategy with MITL models  $\Theta$ . We write  $s_{\text{All}}(\phi)$  as a good proxy for the true performance of the model  $\phi$ . We define the model bias incurred by a subset of models  $\Theta$  as  $B_{\Theta} := \frac{1}{5} \sum_{\phi \in \Theta} |s_{\Theta}(\phi) - s_{\text{All}}(\phi)|$ . We break down the degree of bias  $B_{\Theta}$  into the bias incurred onto oneself (“self-bias”) and the one incurred onto the other models (“non-self-bias”). We quantify the self-bias for a set of models  $\Theta$  to measure the amount of the bias incurred onto oneself:  $\frac{1}{|\Theta|} \sum_{\phi \in \Theta} |s_{\Theta}(\phi) - s_{\text{All}}(\phi)|$ . For example, self-bias for PVSE is  $|76.5 - 76.6| = 0.1$ . The complementary amount of bias, the non-self-bias is computed similarly. For example, PVSE’s non-self-bias is computed as  $|68.0 - 80.1| + |67.7 - 77.4| + |59.5 - 72.4| + |51.7 - 64.3|/4 = 11.8$ .

Figure 6b shows the relationship between the bias quantity and the number of models  $|\Theta|$ . All numbers are averaged over all possible subsets of models of size  $|\Theta|$ . We omit the case with  $|\Theta| = 5$  because all metrics are zero by definition. We have two observations. First, a smaller number of MITL models makes the gap between “self-bias” and “model-bias” larger. This implies that if we use a single model for the MITL annotations, the resulting dataset is highly unlikely to treat the methods differently. Second, the general bias measurements decrease with the number of involved models in the MITL annotation process. For the practical applications, hence, it is advisable to use multiple models to collect the label candidates to verify. In practice, we observe that only three machine annotators (PVSE, PCME and VSRN) achieve better rankings on ECCV mAP@R compared to the COCO R@1 ranking. That suggests that our ECCV Caption is not fully biased towards the selected machine annotators.

## 6 Conclusion

MS-COCO Caption is a popular dataset for evaluating image-text matching (ITM) methods. Despite the popularity, it suffers from the large number of missing positive matches between images and captions. Fully annotating the missing positives with human labor incurs prohibitive costs. We thus rely on machine annotators to propose candidate positive matches and let crowdsourced human annotators to verify the matches. The resulting ITM evaluation benchmark, Extended COCO Validation (ECCV) Caption dataset, contains  $\times 8.47$  positive images and  $\times 3.58$  positive captions compared to the original MS-COCO Caption. We have re-evaluated 25 ITM methods on ECCV Caption with mAP@ $R$ , resulting in certain changes in the ranking of methods. We encourage future studies on ITM to evaluate their models on ECCV mAP@ $R$  that not only focuses on the correctness but also the diversity of top- $k$  retrieved items.

## Appendix

We include additional materials in this document. We first describe the details of our machine annotators (Appendix A), including the explanation of each model (Appendix A.1) and diversity between each model (Appendix A.2). We provide the details of Human Intelligence Tasks (HITs) for ECCV Caption construction (Appendix B), such as detailed questionnaire (Appendix B.1), MTurk worker statistics (Appendix B.2) and the results (Appendix B.3). Appendix C describes the post-processing details, including the full list of invalid items (Appendix C.1) and the examples of ECCV Caption (Appendix C.2). We include more evaluation results in Appendix D, such as training details of re-implemented methods (Appendix D.1), the full results with various evaluation metrics (Appendix D.2), and the full Kendall's  $\tau$  results between evaluation metrics (Appendix D.3). Finally, we provide the full bias analysis in (Appendix E).

## A ECCV Caption Machine Annotators Details

### A.1 Machine annotators

To cover both diversity and practical relevance, we have choose five state-of-the-art cross-modal retrieval models with diverse properties.

- VSRN [13] builds up connections between image regions, and perform reasoning with Graph Convolutional Networks to generates features with semantic relationships. VSRN uses the Faster R-CNN detector [59] as the visual encoder following [64]. VSRN employs the triplet loss [67] with hardest negative mining (HNM) [9].
- PVSE [14] learns a one-to-many function to solve ambiguous matching by one-to-one function. PVSE is a multi-headed model, focusing on diverse matching between two diverse concepts. PVSE also employs the triplet loss with HNM as VSRN.
- PCME [20] is a stochastic model for learning many-to-many correspondences in multi-modal matching tasks. PCME is trained by a probabilistic matching objective function based on the pair-wise matching loss.
- ViLT [30] is a vision-language pretraining method with massive paired data (4.1M images and 9.9M captions). While other methods have separated text and visual backbones, ViLT has a unified shared Transformer [58] backbone for text and visual modalities.
- CLIP [24] is a contrastive approach for massive but noisy associations and shows powerful zero-shot classification performances. CLIP is trained with 4M image and caption pairs. We use the ViT-B/32 CLIP, the largest one when we start the annotation process.

PVSE, VSRN and PCME use pre-trained visual backbones (ImageNet-trained ResNet, Visual Genome [68]-trained Faster R-CNN) and only use COCO Caption dataset as the training dataset. We use the official weights provided by the authors, except for PCME. We re-train PCME with CutMix [61] pretrained ResNet-152. This slightly boosts the original performances. We illustrate the example retrieved images by each model in Figure A.1.

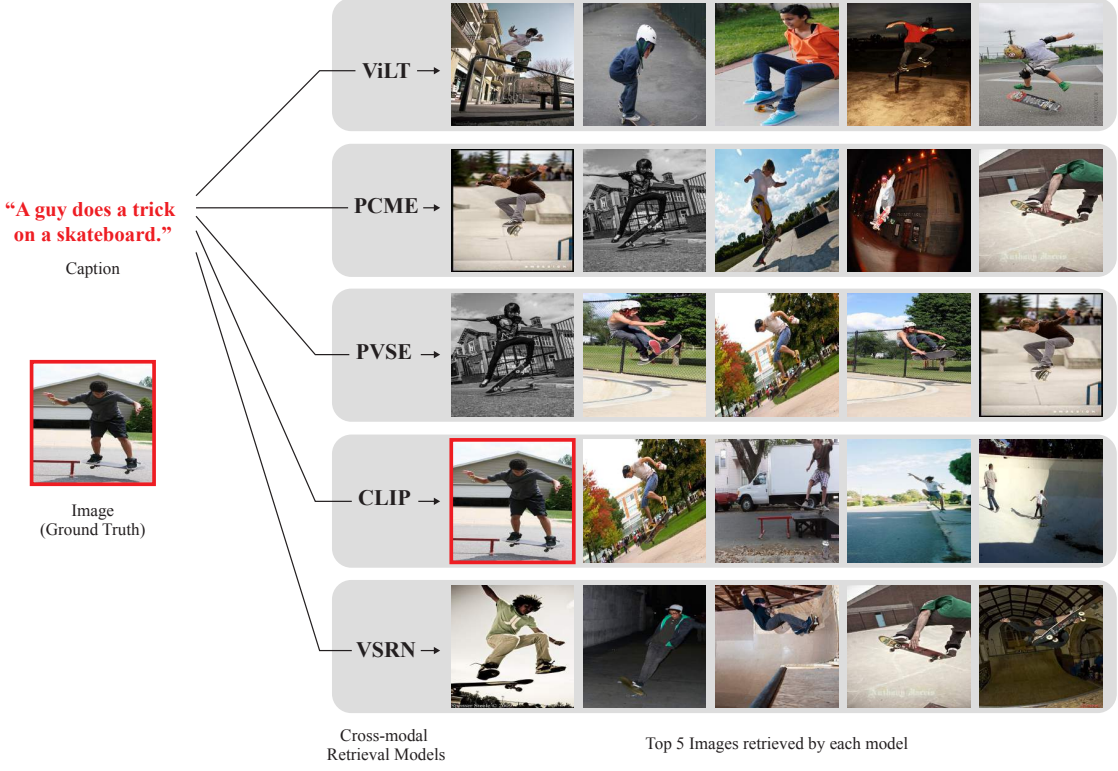


Figure A.1: **Example retrieved images by the machine annotators.** For the given caption ("A guy does a trick on a skateboard."), we show the top-5 images retrieved by models. The matched pair in the dataset is denoted by red boxes.

	PVSE	VSRN	PCME	ViLT	CLIP
PVSE	-	0.266	0.430	0.089	0.088
VSRN	0.266	-	0.260	0.060	0.049
PCME	0.430	0.260	-	0.110	0.120
ViLT	0.089	0.060	0.110	-	-0.013
CLIP	0.088	0.049	0.120	-0.013	-

	PVSE	VSRN	PCME	ViLT	CLIP
PVSE	-	4.52	3.87	5.95	6.24
VSRN	4.50	-	4.47	5.45	5.97
PCME	3.87	4.50	-	5.79	6.20
ViLT	5.79	5.19	5.78	-	6.18
CLIP	6.16	5.81	6.12	6.03	-

(a) **Model similarity analysis by Kendall's  $\tau$ .** A higher score means that two models are more correlated.

(b) **Model similarity analysis by the average ranking.** A smaller rank means that two models are more similar.

Table A.1: **Model similarity analyses.** We measure similarities between the machine annotators in two different ways. (a) We measure the ranking correlations using Kendall's  $\tau$ ; 1.0 means two lists are identical, -1.0 indicates two lists are strongly disagreed each other. (b) We measure the average rankings of the image retrieved by a model for other models. Each row indicates the average ranking of the top-1 retrieved image of the row model for other column models.

## A.2 Diversity between machine annotators

We illustrate the quantify of the diversity between machine annotators by their retrieved items in Table A.1. We retrieve 25 images by each model from the COCO validation captions, and measure (1) Kendall's  $\tau$  (Table A.1a), and (2) the average ranking of the top-1 retrieved items by a model of another model.

Table A.1a shows the Kendall's rank correlation coefficients (Kendall's  $\tau$ ) between the models. Kendall's  $\tau$  is computed on two ranked lists  $[x_1, x_2, \dots, x_n]$  and  $[y_1, y_2, \dots, y_n]$ . We say that two pairs  $(x_i, x_j)$  and  $(y_i, y_j)$ , agree if either  $(x_i > x_j \text{ and } y_i > y_j)$  or  $(x_i < x_j \text{ and } y_i < y_j)$ . Kendall's  $\tau$  is computed by  $\tau = \frac{\#\text{agreed pairs} - \#\text{non-agreed pairs}}{\#\text{all pairs}}$ .

# HITs / worker	# Workers	# Submit. HITs	# Approv. HITs	Approve ratio
1	599	599	459	76.6%
$1 < \text{and} \leq 5$	254	681	535	78.6%
$5 < \text{and} \leq 10$	61	475	374	78.7%
$10 < \text{and} \leq 15$	23	297	216	72.7%
$15 < \text{and} \leq 25$	21	411	285	69.3%
$25 <$	12	506	293	57.9%

Table B.1: **MTurk worker statistics.** The number of the unique workers, the submitted HITs, the approved HITs and the average approve ratio by the number of completed HITs are shown.

## B Human Intelligence Tasks (HITs) for ECCV Caption Construction

### B.1 HIT details

The example HIT for crowd workers is shown in Figure B.1. Each of the 20 questions in the HIT ask the workers to select the degree of belief that the given image-description pair is a positive match. We have designed the HITs in such a way that not only the positivity of the match is recorded, but also the degrees and rationales for the workers’ judgments are collected. Workers can choose among “100% YES”, “Partially YES, but”, “Mostly NO, because”, and “100% NO”. Here, we use four choices instead three level (“YES”, “Not Sure”, and “NO”) to avoid encouraging the workers to select “Not Sure” for all questions. If a worker chooses “Partially YES, but” or “Mostly NO, because”, then they are asked further questions on the rationale behind their uncertainty. Four possible shortcomings for the image-description match are presented as choices: “the description describes concepts that *do not appear* in the image”, “the description *does not describe* the main concepts in the image”, “the description describes the main concepts in *a wrong way*”, and “the description is grammatically incorrect”. Finally, if a worker thinks the description describes the image in a wrong way, we ask *how* the description is wrong. The possible choices here (*e.g.*, quantity, color, ...) have been crystallized from an internal, preliminary study.

We make two separated HITs for the annotation process. In the first stage, we verify the results of the image-to-caption retrieval results of five models. We also ask the crowd workers to justify their answer if they choose “Partially YES” or “Mostly NO”. In the second stage, we verify the results of the caption-to-image retrieval results of the models. After we analyzed the first HITs, we have concluded that the justification stage is not highly useful as our expectation. We omit the justification questions in the second stage for reducing annotation costs. The first annotation round was between 23rd Aug 2021 to 7th Sep 2021. During the first stage, 1,000 HITs are verified by human annotators. The second stage was between 24th Jun 2022 to 10th Feb 2022, and 1,160 HITs are verified during this stage.

### B.2 MTurk workers

Before launching the crowdsourcing on AMT, we have conducted an in-lab study involving 70 HITs and 27 workers for 4 days. We have observed that if workers continuously complete HITs, the average elapsed time per HIT is about 4 to 8 minutes. Based on this estimate, we have set the compensation level for each HIT to \$1.4 so that a worker can earn \$15 per hour in the first stage. For the second stage, we have set the compensation level for each HIT to \$0.65, based on the similar in-lab study without justification questions. The final costs including platform fees for the first and the second stages are \$1.65 and \$0.78, respectively.

In the main crowdsourcing phases, crowd workers are recruited through AMT. The detailed statistics for workers are shown in Table B.1. Overall, 970 unique workers have completed 2,969 unique Human Intelligence Tasks (HITs), while 807 HITs of them (37.3%) have been rejected by our qualification process. The average elapsed time for each HIT of the first and second annotation phase are 9.5 and 13.8 minutes, respectively. The average HITs per worker is 3.06.

### B.3 MTurk results

We summarize the results of the crowdsourced annotations, corresponding to 2,160 approved HITs on MTurk, in Table B.2 and Table B.3. In Table B.2, we show the ratios of “Yes”, “Weak yes”, “Weak no” and “No” for different models and rankings. Here, we observe that weaker results (*i.e.*, worse ranked pairs)

**Image:**



**Description:** A gray horse grazing in a field on a sunny day.

(a) Is the image correctly described?

100% YES  Partially YES, but...  Mostly NO, because...  100% NO

--- Explanation: the description and the image is almost matched but it is partially wrong.

(b) What are the shortcomings of the description? Choose all that apply.

It describes objects/concepts that *do not appear* in the image  
 It *does not describe* the main objects/concepts in the image.  
 It describes the main objects/concepts in the image, *but in a wrong way* (incorrect gender, quantity, color, action, ...).  
 It is grammatically incorrect or otherwise confusing.

--- Explanation: all concepts in the caption is in the image; the main object is horses; it is grammatically correct; but its description is partially wrong.

(c) If the description explains the image in a wrong way, which concept is not correct?

Quantity  Color; Texture; Material  Species (or object class)  Gender  Age  Action  Emotion  Location  
 Orientation  Others:

--- Explanation: There are **two horses** with gray and white.

**Figure B.1: Example question in a MTurk HIT.** The question asks whether the image is correctly described. If unsure (“Partially YES, but ...” or “Mostly NO, because ...”), the question prompts the worker to provide the rationale. There are 20 of such questions in each HIT.

have lower “Yes” and “Weak yes” ratios. For example, the annotation results for PCME show that the “Yes” ratios monotonically decrease as the rank goes down: 52.3% for the most similar pairs, but 27.8% for the least similar pairs. Interestingly, we observe that the average ratio of “Yes” + “Weak yes” for the top-1 retrieved items exceed 80% for all five models (*e.g.*, 86.0% for VSRN), while the R@1 score of each model is known to less than 60% (See Table 4 in the main paper).

From the table, we observe that by letting annotators verify more similar pairs by machines, the annotation process becomes more efficient, *i.e.*, we can acquire the same amount of positive annotations with less number of human verification. However, as we will discuss in depth later, we emphasize that the model power is not only factor to consider: model biases emerge in MITL-produced datasets regardless of the strength of the model.

Rank	PVSE				VSRN			
	Yes	Weak yes	Weak no	No	Yes	Weak yes	Weak no	No
1	52.3	31.7	11.2	4.7	54.4	31.6	10.0	4.0
2	39.0	36.7	16.7	7.5	39.9	37.6	15.8	6.7
3	34.5	36.9	18.0	10.6	36.6	36.8	17.6	9.0
4	30.9	39.2	19.6	10.4	33.2	38.1	17.6	11.1
5	28.0	39.2	20.5	12.3	30.4	38.6	19.0	12.0
Avg.	36.8	36.8	17.3	9.1	38.8	36.6	16.0	8.6

Rank	PCME				ViLT			
	Yes	Weak yes	Weak no	No	Yes	Weak yes	Weak no	No
1	52.3	33.2	10.4	4.2	47.6	33.7	12.0	6.7
2	39.8	37.2	15.1	7.9	36.6	33.5	19.7	10.2
3	35.6	39.0	17.5	7.9	30.3	35.6	20.2	13.9
4	31.9	37.8	21.1	9.2	26.7	35.6	22.8	14.9
5	27.8	40.0	21.5	10.6	25.8	35.6	22.5	16.1
Avg.	37.4	37.5	17.2	8.0	32.9	34.8	19.7	12.5

Rank	CLIP			
	Yes	Weak yes	Weak no	No
1	50.5	33.5	12.0	3.9
2	35.3	38.5	18.0	8.2
3	33.8	39.9	16.1	10.1
4	31.0	38.6	18.0	12.5
5	28.4	39.8	20.2	11.6
Avg.	36.0	38.0	16.8	9.2

Table B.2: **Model-wise annotation overview.** The percentages of “100% YES”, “Partially YES”, “Mostly NO” and “100% NO” for each model and each ranking are shown. For example, the first row indicates the annotation results for the top-1 retrieved image and description pairs.

We additionally show the rationales for the uncertain matches and the specification of the errors in Table B.3. We observe that the models result in similar patterns in the annotations’ rationale and specification of errors. Finally, by our annotation process, the average number of “100% YES” and “Partially YES” images for each caption is 8.3 and 7.1, respectively. It is remarkable since original COCO annotations allow only one image to be positively paired to a caption, revealing the massive amount of missed positive matches.

## C ECCV Caption Post-processing Details

### C.1 The full list of invalid captions and images

In this subsection, we list up the invalid captions and images in the original COCO test split. We filter the invalid captions by the following process: (1) We first list up the “true positive” (*i.e.*, the positive pairs in the original COCO test set) annotated by “100% No” items by Turkers or CxC [31]. (2) We manually validate the items into two categories: totally wrong captions (*e.g.*, “I don’t know” captions) and semantically incorrect captions (*e.g.*, “A group of birds flying above the beach” for an image with kites). The full list of invalid captions with their COCO caption ids are as follows:

- 607516 The first picture is blank all the time on purpose.
- 607486 Why is my first one a blank every time.
- 433639 There is no image here to provide a caption for.
- 248212 I am unable to see an image above.
- 469834 There is no image here to provide a caption for.
- 462530 I really cant see this image very well.

	Not in image	Not in caption	Incorrect object description	grammar error
PVSE	30.4	17.5	48.0	4.1
VSRN	30.1	18.4	46.5	5.0
PCME	31.6	17.9	46.1	4.4
ViLT	31.2	18.9	45.7	4.2
CLIP	28.8	18.5	47.1	5.6
Avg.	30.4	18.2	46.7	4.7

(a) **Shortcomings by models.**

	Quantity	Color	Species	Gender	Age	Action	Emotion	Location	Orientation	Others
PVSE	25.7	20.1	11.9	5.4	2.2	14.9	0.9	3.4	12.1	3.2
VSRN	23.8	20.1	12.7	4.0	1.7	15.5	1.2	4.3	13.6	3.0
PCME	24.8	20.9	12.1	5.6	2.1	14.3	0.8	4.2	12.1	3.1
ViLT	24.9	20.8	11.2	6.3	2.1	14.9	0.9	3.7	12.8	2.4
CLIP	27.2	19.7	13.5	3.5	1.7	14.5	1.1	3.9	11.3	3.5
Avg.	25.3	20.3	12.3	5.0	2.0	14.8	1.0	3.9	12.4	3.0

(b) **Detailed errors by models.**

Table B.3: **Error types.** The percentage of the error types by models. There is no statistical significant difference by models.

- 469102 There is no image to be reviewed on this hit.
- 743575 There is no image showing on this page to describe.
- 246706 I am unable to see an image above.
- 61717 There is no picture here to describe with a caption.
- 500797 I am unable to see the image above.
- 19273 There is no image for me to write about.
- 630298 There is no image to provide a caption for.
- 576409 I am unable to see the image above.
- 390637 I am unable to see an image above.
- 296557 There is no image here to provide a caption for.
- 450553 I am unable to see an image above.
- 44809 blank image with no pictures available to write about

We also show the list of semantically incorrect captions as the follows:

- 610564 An individual is in the open view in the image.
- 359139 I cant tell if the bears may be fighting or kissing.
- 218995 A baseball player hugging another player as lovers do.
- 609235 Individuals are up and doing something fun today.
- 143250 The bar of the small bathroom has many remotes on it.
- 375316 A photo duplicated a few times and put together.
- 712683 Talk about a bad hair day, his is frightful.
- 75083 A group of birds flying above the beach.
- 625605 It is always wise to have bottles of water on hand in case of an emergency.
- 620511 If the motorcycle brakes down, the bicycle will be good transportation.
- 613949 A full view of an outdoor space with many things to see.
- 129825 A picture of a comment that is open.



Figure C.1: **An example image of semantically wrong captions.** We annotate “A group of birds flying above the beach” as a wrong caption of the figure, while the other captions are available in Figure C.2.

- 605566 There is a room with various items in the picture.
- 634829 That thing is really red and slow lol

Finally, we omit `COCO_val2014_000000578492.jpg` from our test set, where the image is duplicated to training images: `COCO_train2014_000000388662.jpg` and `COCO_train2014_000000397819.jpg`.

## C.2 More examples of ECCV Caption

We illustrate the samples from ECCV Caption in Figure C.2.

## D More Evaluation Results on ECCV Caption

### D.1 Training details

We follow the implementation details by Chun *et al.* [20]. We use the AdamP [70] optimizer and cosine annealing learning rate scheduling [71]. For re-implemented VSE, PVSE and PCME, we use the pre-trained ResNet-152 backbone and pre-trained Glove vectors following previous studies [9, 14, 20]. We use two-stage training scheme that includes “pre-training” (freezing pre-trained backbones, but only updating the additional modules) and “fine-tuning” (updating the whole parameters). The models are pre-trained during 30 epochs and fine-tuned during 30 epochs. For the improved PCME, we use the ResNet-152 model trained with the CutMix [61] augmentation for achieving better R@1 accuracies.

### D.2 Full table

Table D.1 and Table D.2 show the full results of each model for image-to-text retrieval tasks and text-to-image retrieval tasks, respectively.

### D.3 Kendall’s rank correlations between metrics

Table D.3 shows the full results of Kendall’s rank correlations between metrics. We observe that Recall@ $k$  metrics are highly correlated (usually larger than 0.8).

## E Analysis of Biases in MITL

### E.1 Image caption matching problem to general annotation tasks

Many real-world applications are powered by state-of-the-art machine learning (ML) models shown to exceed human-level performances in tasks such as natural language understanding [72] and image classification [51, 73]. However, previous studies have shown that two conditions must be met for these models to perform well: massive training data and quality annotations. For example, large datasets that



Kites being flown along the coast line in the morning  
 People watch multi colored items fly above the beach.  
 A beach where people are flying kites at sunset.  
 A crowd of people flying kites on the beach.  
 Dozens of kite skiers out in the ocean  
 People in the water and parachutes overhead.  
 Many different sails flying over a large body of water.  
 There are many large kites flying above the beach.  
 Kites are flying over people on a beach.  
 A bunch of kites flying in the sky on the beach.  
 Several gliders floating on the ocean next to an island.  
 A couple flying a kite at dusk on the seaside.  
 People on a sunny beach flying various kites



The tennis player is extending his reach to hit the racket.  
 A man swings his racket to hit a tennis ball.  
 A tennis player swinging the rackets towards the ball.  
 A man that is standing up and has a tennis racket.  
 A man lunging to hit a tennis ball in a match.  
 A male tennis player walking on the tennis court.  
 A man on a court swinging a racket at a ball.  
 The man is playing tennis with a racket.  
 A man standing on a tennis court holding a racquet.  
 A man on a tennis court trying to hit the ball.  
 A man taking a swing at a tennis ball.  
 A man taking a swing at a tennis ball.  
 A man throwing a tennis ball in the air for him to hit with his racket.  
 A man hitting a tennis ball with a racquet.  
 A man with a tennis racket is running on a court.  
 A man swinging his racket to hit the ball.  
 The tennis player is hitting the ball with his racket.  
 A tennis player caught jumping up to hit the ball.  
 A man is holding a tennis racquet prepared to hit the incoming ball.  
 A man holding a tennis racquet as a ball clears the net.  
 A man with a racket prepares to hit a tennis ball.  
 A man in shorts and a long sleeve shirt playing tennis.

A man stands on a tennis court hitting a ball with a racket.  
 A man plays a game of tennis during the day.  
 A man with a tennis racket swings at a tennis ball.  
 A man with a tennis racket on a court.  
 A man playing tennis on the tennis court.  
 A person hitting a tennis ball with a tennis racket.  
 A man playing tennis and holding back his racket to hit the ball.  
 A male tennis player swinging his tennis racket.  
 A man swinging at a tennis ball with a tennis racket.  
 A person hitting a tennis ball with a tennis racket.  
 A man on a tennis court that has a racquet.  
 A man in a head band hits a tennis ball.  
 A man standing on top of a tennis court holding a racquet.  
 A male in a blue shirt playing tennis on a tennis court.  
 A man holding a tennis racket on a tennis court.  
 A tennis player swinging a racket at a ball.  
 A man holding a racket on top of a tennis court.  
 A boy hitting a tennis ball on the tennis court.  
 A man on a court swinging a tennis racket.  
 A man in white shirt and shorts playing tennis.  
 A guy in a maroon shirt is holding a tennis racket out to hit a tennis ball.  
 A person hitting a tennis ball with a tennis racket on a tennis court.  
 The man is playing tennis on the court.



Some zebras are seen grazing in the field.  
 Four adult zebra are grazing on a field of grass.  
 Four zebras are grazing on grass in a pasture.  
 Four zebras eating grass on a field.  
 A herd of zebra standing on top of a lush green field.  
 These four zebra are walking in a field.  
 There is a herd of zebra standing around.  
 A herd of zebras walking through the grass.  
 Clouds with a rainbow in the sky of an open field with zebras grazing on the grass.  
 Several zebras in an open area during a not so sunny day.  
 A group of zebras that are standing in the grass.  
 A group of zebras in a grassy and forested area.  
 Four zebras are grazing at a nature reserve.  
 Zebras graze in a grass and bush fenced enclosure.  
 There are some zebras standing in a grassy field.  
 The zebra is standing in the field with the other animals in the background.  
 Four zebras standing in the grass on a cloudy day.  
 Four zebras walking in a grassy area.

A herd of zebras stand on a pathway near brown grass.  
 Zebras graze on the plains with trees in the background.  
 Three zebras and two other animals grazing.  
 Several zebras walking the terrain of hills and mountains.  
 Two zebras in some brown and green grass and some bushes.  
 A herd of zebras grazing with a rainbow behind.  
 A herd of zebra grazing on a dry grass field.  
 Herd of five zebras grazing in a field.  
 Two black and white zebras and some green grass and trees.  
 A group of zebra standing on top of a dry grass field.  
 A zebra is standing outside on the grass by itself.  
 Three zebra in the middle of a field with a body of water in the distance.  
 Zebras grazing on sparse grass in an enclosure at an animal park.  
 A herd of zebras grazing in a field and a rainbow.  
 A group of zebras are on some grass with trees and bushes behind them.  
 A few deer and a zebra on a grass field.  
 Several zebras eat the green grass in the pasture.

**Query: Boats are traveling in the large open water.**

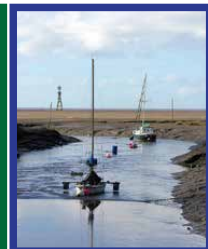


Figure C.2: Example sample from ECCV Caption. Positive captions and images in ECCV Caption. **Red:** original positive. **Green:** annotated as “100% Yes”. **Blue:** annotated as “Weak Yes”.

	ECCV			CxG		COCO 1K		COCO 5K		
	mAP@R	R-P	R@1	R@1	R@1	R@5	R@1	R@5	PMRP	
ResNet-152 [51] image encoder + Bi-GRU [57] text encoder										
VSE0 <sup>†</sup>	14.92	26.05	44.73	26.92	48.50	81.74	24.76	53.82	51.54	
VSE++ <sup>†</sup>	24.45	36.51	64.31	43.66	66.86	91.34	41.52	72.10	59.58	
PVSE K=1	23.40	35.56	62.57	43.88	66.70	90.94	41.76	72.96	58.80	
PVSE K=2	26.72	39.24	65.03	46.08	68.42	91.26	44.10	73.38	60.69	
PCME	26.24	38.65	65.50	46.22	68.78	91.42	44.26	73.52	60.87	
PCME (CutMix) <sup>†</sup>	28.55	41.23	68.75	47.14	68.72	92.58	45.04	75.12	61.85	
Region features based on Bottom-up Attention [64] and SCAN [11]										
VSRN	30.77	42.89	73.83	55.06	76.20	94.76	53.02	81.12	62.41	
VSRN + AOQ	30.70	42.61	73.12	56.86	77.50	95.44	55.14	83.30	62.47	
CVSE	28.11	40.14	69.23	52.92	74.14	94.94	51.00	79.58	62.23	
SGR	27.24	39.15	71.05	58.80	77.26	95.94	57.24	83.18	61.98	
SAF	27.36	39.30	71.05	56.98	78.06	95.84	55.48	83.82	62.00	
VSE infty (BUTD region)	31.36	42.78	74.86	60.12	79.64	96.38	58.34	85.32	62.98	
VSE infty (BUTD grid)	31.68	43.08	76.53	60.64	80.42	96.78	59.10	85.90	62.79	
VSE infty (WSL grid)	34.80	45.41	81.05	67.88	84.50	98.06	66.38	89.34	64.13	
Large-scale Vision-Language pretraining										
CLIP ViT-B/32	22.39	32.61	66.06	51.68	69.26	90.92	50.14	75.00	54.40	
CLIP ViT-B/16	23.67	33.96	68.68	53.84	71.56	91.40	52.30	76.78	56.46	
CLIP ViT-L/14	24.00	33.84	71.37	57.98	74.20	92.84	56.32	79.32	59.79	
VinVL (zero-shot)	16.17	27.31	49.64	37.06	58.06	87.54	35.18	64.36	36.80	
VinVL	34.56	44.39	83.35	75.74	88.14	98.32	74.66	92.58	75.73	
ViLT (zero-shot)	23.22	33.64	65.34	58.24	77.10	95.12	56.70	82.54	57.26	
ViLT	27.50	38.57	73.35	62.76	80.76	96.28	61.50	86.26	62.65	
BLIP	36.02	44.56	88.50	82.68	92.28	98.96	81.90	95.38	82.32	
Different negative mining (NM) strategies										
PVSE K=1, Sum triplet <sup>†</sup>	22.26	34.97	56.70	37.18	60.42	89.24	35.16	66.32	37.27	
PVSE K=1, SHM <sup>†</sup>	25.24	37.67	64.00	43.24	66.12	91.36	41.14	71.64	42.90	
PVSE K=1, HNM <sup>†</sup>	25.24	37.75	64.55	44.78	67.18	91.94	42.70	73.56	45.36	

Table D.1: **Re-evaluating VL models: Image-to-text retrieval results.**

consist of well-curated 1M images [74], 3.5B Instagram photos [75, 76], 300M web photos [60], 400M captioned images [24], 1.8B noisy captioned images [77], 15M hierarchically structured images [60, 78], and synthetic images [61, 79–81] are the key factors behind the corresponding models’ success. Moreover, the annotation quality is equally important for the model performances. Mahajan *et al.* [75] showed that training on 940M images with well-processed 1.5k labels results in a model comparable to training on 3.5B images with noisy and weak 17k labels; both models show 84.2% ImageNet-1K top-1 accuracy.

An emerging pattern for obtaining quality labels for a large dataset is pipelining a machine learning model and human annotators. Expert human annotators are reliable and produce high-quality label, but they are costly to accommodate. Strong machine annotators are relatively inexpensive, but they result in low-quality and unreliable annotations. One popular method of combining the two is feeding human annotators with machine learning model’s outputs. For example, a model suggests annotations (*e.g.*, candidates of labels [49], estimated boxes [49], estimated segmentation maps [42], estimated descriptions [82]) for the given data point, and the annotators only need to confirm or fix the labels given by the machine annotators. This approach is commonly used for building a large-scale dataset, such as OpenImages [42, 49], e-Vil [82].

While rich body of discussions are available for building annotation interfaces and crowdsourcing workflows, we still lack a good understanding of the impact the underlying machine learning models have on the annotators and on the annotation results. In this research, we specifically examine the downstream effects of a common practice where researchers and practitioners consider only one “strong” model in the machine-in-the-loop annotation pipeline. This can be problematic because different models not only

	ECCV			CxG		COCO 1K		COCO 5K		
	mAP@R	R-P	R@1	R@1	R@5	R@1	R@5	PMRP		
ResNet-152 [51] image encoder + Bi-GRU [57] text encoder										
VSE0 <sup>†</sup>	30.41	40.48	66.37	21.56	39.95	74.71	19.78	46.12	42.36	
VSE++ <sup>†</sup>	45.57	54.49	81.91	32.24	52.76	84.79	30.05	60.11	48.94	
PVSE K=1	44.55	53.41	83.93	32.88	53.49	85.11	30.64	61.37	48.32	
PVSE K=2	53.8	60.6	88.44	34.27	54.91	86.5	32.15	62.79	50.36	
PCME	47.97	56.99	84.08	33.95	54.65	86.25	31.8	62.17	52.54	
PCME (CutMix) <sup>†</sup>	54.92	61.66	88.59	36.26	56.7	87.08	33.97	63.77	53.46	
Region features based on Bottom-up Attention [64] and SCAN [11]										
VSRN	53.78	60.78	89.19	42.63	62.77	89.71	40.46	70.58	48.47	
VSRN + AOQ	51.17	58.68	89.94	43.34	63.46	90.5	41.14	71.5	50.36	
CVSE	46.59	54.88	84.16	38.71	59.88	89.29	36.6	68.04	50.74	
SGR	44.35	52.93	86.49	42.39	62.06	89.56	40.47	69.64	51.84	
SAF	44.55	53.07	85.66	42.18	62.24	89.53	40.12	69.73	52.42	
VSE infty (BUTD region)	49.56	57.16	90.17	44.67	64.79	91.41	42.41	72.67	50.31	
VSE infty (BUTD grid)	49.12	57.1	89.49	46.29	66.42	92.1	44.09	74.1	50.94	
VSE infty (WSL grid)	50.02	57.45	91.82	53.7	72.04	93.92	51.64	79.34	51.16	
Large-scale Vision-Language pretraining										
CLIP ViT-B/32	31.11	41.2	68.09	32.26	49.68	79.29	30.42	55.96	50.69	
CLIP ViT-B/16	34.82	44.01	73.42	34.67	52.47	80.86	33.07	58.42	51.80	
CLIP ViT-L/14	31.96	41.76	72.97	38.3	55.46	82.29	36.55	61.05	52.82	
VinVL (zero-shot)	28.19	38.54	60.74	30.41	50.15	80.37	28.96	56.99	37.55	
VinVL	47.06	54.71	92.19	59.77	76.62	95.15	58.12	83.2	46.79	
ViLT (zero-shot)	30.46	39.97	72.65	42.45	62.26	90.7	40.56	70	51.90	
ViLT	41.66	49.97	82.27	44.68	64.73	91.84	42.85	72.76	53.11	
BLIP	45.01	52.3	93.47	65.92	79.95	95.8	64.32	85.73	53.15	
Different negative mining (NM) strategies										
PVSE K=1, Sum triplet <sup>†</sup>	44.41	53.91	79.28	28.2	49.3	83.68	26.13	56.4	52.42	
PVSE K=1, SHM <sup>†</sup>	48.02	57.05	83.93	33.09	53.57	85.45	30.86	60.83	49.91	
PVSE K=1, HNM <sup>†</sup>	46.28	55.24	82.81	33.25	54.02	85.4	31.06	61.26	48.99	

Table D.2: **Re-evaluating VL models: Text-to-image retrieval results.**

show different results to the human annotators, but also in different orders, bring the impartialness of the annotated dataset towards any particular model to the surface. In other words, the machine-in-the-loop annotations are not stable across model choices.

As a realistic scenario for utilizing ML models to aid annotators, we consider the COCO Caption matching task [1, 2] that matches each image with sentences in a large database of captions. Due to the sheer bulk of the involved databases (123,287 images and 616,767 captions), it is infeasible for annotators to search through the matching caption. Instead, for each image, we use model-based ranking of possible captions to greatly reduce the search space for annotators. We have conducted studies with five state-of-the-art image-text matching models. Our COCO Caption matching task can be seen as the extreme version of the class label selection task where the number of possible classes is as large as the number of possible descriptions.

A decent overview of the image annotation tools is provided by Sager *et al.* [83]. The annotation task is determined along two axes: the types of inputs and the expressiveness of the labels. This paper focuses on the image inputs, one of the most frequently annotated type of data. The expressiveness and complexity of labels are directly related to the learning task being addressed. Tagging images with class labels is arguably the most common and basic form in the spectrum of label expressiveness. In the other extreme, we have the *image-caption matching task*: given an image, annotator has to search through the database of descriptions to find the one that best matches the image [2]. The caption matching task is of the same nature as image tagging: one needs to find the correct label in a list of possible labels. However, the candidate space for the

	COCO 1K		COCO 5K		CxC	ECCV		COCO
	R@1	R@5	R@1	R@5	R@1	R@1	R-P	PMRP
COCO 1K R@1	-	<b>0.87</b>	<b>0.89</b>	<b>0.97</b>	<b>0.89</b>	0.72	0.39	0.47
COCO 1K R@5	<b>0.87</b>	-	0.79	<b>0.88</b>	0.79	<b>0.81</b>	0.49	0.58
COCO 5K R@1	<b>0.89</b>	0.79	-	<b>0.89</b>	<b>1.00</b>	0.65	0.30	0.39
COCO 5K R@5	<b>0.97</b>	<b>0.88</b>	<b>0.89</b>	-	<b>0.89</b>	0.75	0.41	0.50
CxC R@1	<b>0.89</b>	0.79	<b>1.00</b>	<b>0.89</b>	-	0.65	0.30	0.39
ECCV R@1	0.72	<b>0.81</b>	0.65	0.75	0.65	-	0.65	0.74
ECCV R-P	0.39	0.49	0.30	0.41	0.30	0.65	-	<b>0.90</b>
ECCV mAP@R	0.47	0.58	0.39	0.50	0.39	0.74	<b>0.90</b>	-
PMRP	0.45	0.39	0.45	0.43	0.45	0.29	0.17	0.20

Table D.3: **Rank correlations between evaluation metrics.** Higher  $\tau$  denotes two rankings are highly correlated, while  $\tau$  values near zero denotes two rankings are barely correlated. We highlight the highly correlated pairs ( $\tau > 0.8$ ) with **red** text.

possible labels is exponentially greater for the caption matching task. If the vocabulary size is  $V$  and the lengths of caption sequences are generally  $L$ , the size of the candidate space is as large as  $O(V^L)$ . This contrasts against the number of possible class labels that are generally far smaller than  $V$ .

We consider the image-caption matching as a testbed for analyzing annotation pipelines for two reasons. First, it is highly relevant for the MITL annotation paradigm because it is downright infeasible for humans to browse through the database. Second, it inherits the same tool as image tagging, making our experimental results and analyses transferable to general image tagging tasks.

## E.2 What Do We Mean by “Bias”?

Bias is an overloaded term with multiple senses. We briefly explore its use in relevant fields and make a definition relevant to our paper.

In statistics and machine learning, bias of an estimator or model refers to the mismatch between its average behavior and the true parameter or underlying function [84, 85]. We partially adopt this definition of bias in a broad sense. The annotation pipeline as a whole can be regarded as a mechanism for assigning plausible labels to a given set of images. When we say that the annotation pipeline is “biased”, we refer to the discrepancy between the resulting annotations and the true, underlying labels for the samples.

In human-related studies, like psychology, neuroscience, human-computer interaction, and increasingly in machine learning, the use of “bias” often points to its underlying human factor. Examples include “confirmation bias” where humans favorably select data that serve their purpose [86], “reporting bias” where crucial commonsense knowledge is overlooked [87], and “survivorship bias” where non-surviving cases are under-represented [88]. In our MITL annotation pipeline, we study the *model bias* where models hinder humans from generating an unbiased set of labels by presenting humans with only a selection of the candidate labels deemed correct by the models.

## E.3 Biases in ECCV Caption

Given the crowdsourced labeled image-caption data of ECCV Caption, our aim is to analyze the degrees of bias in them, depending on the underlying model used for machine-in-the-loop (MITL) labeling paradigm. Specifically, we are interested in the model bias, the type of bias that arises because of the pre-selection of plausible samples by the model in the annotation pipeline. We measure the model bias by employing the crowdsourced data as the source for evaluating the cross-modal retrieval models. For a perfectly unbiased data, we shall expect the identical evaluation results (*i.e.*, in terms of the ranking of the methods) across the version of datasets collected with different models. In this section, we introduce the strategy to measure the model bias and present experimental results and analyses.

We measure the model bias in a labeled dataset by examining whether certain versions of datasets behaves favorably to certain models when they are used as the evaluation benchmark. To measure this, we need to introduce the specific evaluation metrics used for measuring the cross-modal retrieval performances. We use *Recall@1* and *R-Precision*.

Recall@1 is the most widely-used metric for reporting the performances of cross-modal retrieval models. To compute it, we first let  $m_i(x)$  be the indicator whether the  $i$ -th retrieved item of the input  $x$  is a positive match.

$$\begin{aligned} m_i(x) &= 1 && \text{if } i\text{-th retrieved item of } x \text{ is a positive match;} \\ m_i(x) &= 0 && \text{otherwise.} \end{aligned} \quad (\text{E.1})$$

Recall@1 measures whether the top-1 retrieved item is a positive match on average:

$$\text{R@1} = \frac{1}{N} \sum_{n=1}^N m_i(x_n). \quad (\text{E.2})$$

Despite its popularity, Recall@1 has a serious shortcoming. As argued by Musgrave *et al.* [29], a high Recall@1 does not always guarantee high-quality retrieval results. Musgrave *et al.* have proposed to use the R-Precision as an alternative metric. Let  $R(x)$  be the total number of matched items for the input  $x$ . Then, R-Precision is defined as follows:

$$\text{R-P} = \frac{1}{N} \sum_{n=1}^N \frac{1}{R(x)} \sum_{i=1}^{R(x)} m_i(x_n). \quad (\text{E.3})$$

Despite its good properties, in practice, it is impossible to use R-Precision for cross-modal retrieval benchmarks because many cross-modal retrieval benchmarks only a few number of (*e.g.*, 1) positive pairs in the dataset. However, as shown in Figure A.1, there actually are many plausible positive pairs missed by the original positive pairs.

We further refurbish the metrics by using the fine-grained degrees of pair positivity provided by the annotators (Appendix B.2), which are not available for conventional cross-modal retrieval datasets. We update the matching function (Equation (E.1)) as follows:

$$\begin{aligned} m_i(x) &= 1 && \text{if } i\text{-th retrieved item of } x \text{ is annotated as "100% YES"} \\ m_i(x) &= 0.5 && \text{if } i\text{-th retrieved item of } x \text{ is annotated as "Partially YES"} \\ m_i(x) &= 0 && \text{otherwise.} \end{aligned} \quad (\text{E.4})$$

We report the modified Recall@1 and R-Precision using the matching function above as the final performance metric for cross-modal retrieval models on our crowdsourced datasets.

Table E.1a and Table E.1b show the model performances on different versions of datasets using one of the MITL models in the pool.

We observe that the model performances on different versions of datasets using one of the MITL models in the pool (results are in Appendix). We observe that the best-performing model for each dataset is the exact model used for the MITL label proposal process, with quite some margin against the other models. This strongly corroborates the existence of model bias in datasets collected with the aid of machine filtering. We further observe that even for models not used for generating the label proposals (*i.e.*, the non-diagonal elements in Table E.1a and Table E.1b), the rankings shift with respect to the underlying MITL model.

This suggests that even when one avoids the direct use of the MITL model for evaluating its own performance (*i.e.*, avoiding the diagonal results), one may still observe unstable evaluation results, where different MITL models arbitrarily favor different models.

A crucial limitation in an analysis of this type is the lack of the *true labels*. The obtained versions of datasets are clearly enhanced versions compared to the original COCO Caption dataset, but they are still heavily affected by the model biases as seen above. To make a better estimate of how far the datasets are from the true labels, we introduce the *multi-model strategy* where the workers verify label proposals generated by more than two of the models involved. More specifically, a multi-model strategy involving models  $\Theta = \{\text{PVSE, PCME}\}$  pools the label proposals from both PVSE and PCME and present them to the human annotators. The rest of the verification process is identical as before. The intuition is that the dataset built with the multiple models will be much closer to the true labels for the image-caption matches. In the extreme case, we have the *all-model strategy* involving all five models considered in this work. See the “All” columns in Table E.1a and Table E.1b for the corresponding results.

Based on this intuition, we suggest an additional metric to measure the distance between a version of dataset and the all-model dataset, which is deemed to contain the labels that are closest to the true labels.

Models	Models used for annotations					
	PVSE	VSRN	PCME	ViLT	CLIP	All
PVSE	<b>76.5</b>	63.6	67.6	45.3	42.0	76.6
VSRN	68.0	<b>80.1</b>	69.0	51.1	47.2	<b>80.1</b>
PCME	67.7	64.3	<b>77.3</b>	46.0	44.1	77.4
ViLT	59.5	59.8	58.8	<b>62.0</b>	<b>49.3</b>	72.4
CLIP	51.7	51.5	52.6	42.8	<b>49.3</b>	64.3

(a) Text-to-Image Recall@1.

Models	Models used for annotations					
	PVSE	VSRN	PCME	ViLT	CLIP	All
PVSE	<b>53.5</b>	39.4	42.1	30.1	31.3	42.1
VSRN	41.8	<b>55.9</b>	41.6	33.8	35.9	<b>43.2</b>
PCME	42.9	39.9	<b>54.8</b>	31.8	33.8	43.1
ViLT	34.0	34.5	33.9	<b>45.5</b>	37.0	35.8
CLIP	31.0	31.5	31.9	29.6	<b>39.6</b>	32.1

(b) Text-to-Image R-Precision.

Table E.1: **Model performances vs. different annotation processes.** Each row indicates performances of the same model by different annotation strategies: using the annotations filtered by a specific model. For example, the first column of the tables shows the model performances by only using “PVSE” filtered annotation. “All” denotes the full annotations are used. The bold numbers denote the best model performances for each annotation strategy, where the best performed model and the model used for the annotation strategy are the same in all experiments.

We define  $s_\Theta(\phi)$  as the performance of the model  $\phi$  evaluated upon the dataset built with the multi-model strategy with MITL models  $\Theta$ . We write  $s_{\text{All}}(\phi)$  as a good proxy for the true performance of the model  $\phi$ . We define the model bias incurred by a subset of models  $\Theta$  as

$$\mathcal{B}_\Theta := \frac{1}{5} \sum_{\phi \in \text{All}} |s_\Theta(\phi) - s_{\text{All}}(\phi)| \quad (\text{E.5})$$

where  $\text{All} = \{\text{PVSE, VSRN, PCEM, ViLT, CLIP}\}$ . For example,  $\mathcal{B}_{\{\text{PVSE}\}}$  using Recall@1 (Table E.1a) is computed as follows:

$$\begin{aligned} \mathcal{B}_{\{\text{PVSE}\}} = & (|76.5 - 76.6| + |68.0 - 80.1| + |67.7 - 77.4| \\ & + |59.5 - 72.4| + |51.7 - 64.3|) / 5 = 9.5 \end{aligned} \quad (\text{E.6})$$

We break down the degree of bias above into the bias incurred onto oneself (“self-bias”) and the one incurred onto the other models (“non-self-bias”). We quantify the self-bias for a set of models  $\Theta$  to measure the amount of the bias incurred onto oneself:  $\frac{1}{|\Theta|} \sum_{\phi \in \Theta} |s_\Theta(\phi) - s_{\text{All}}(\phi)|$ . For example, self-bias for PVSE is  $|76.5 - 76.6| = 0.1$ . The complementary amount of bias, the non-self-bias is computed similarly. For example, PVSE’s non-self-bias is computed as  $|68.0 - 80.1| + |67.7 - 77.4| + |59.5 - 72.4| + |51.7 - 64.3| / 4 = 11.8$ .

We plot the degrees of the biases, measured with  $\mathcal{B}_\Theta$ , self-bias, and non-self-bias in Figure E.2. We have experimented with changing the numbers of models  $|\Theta|$ . All numbers are averaged over all possible subsets of models of size  $|\Theta|$  (e.g., if  $|\Theta| = 2$ , the result is the average of  $n(n - 1)/2$  numbers). We omit the case with  $|\Theta| = 5$  because all metrics are zero by definition.

We have two observations. First, the smaller number of MITL models make the gap between “self-bias” and “model-bias” larger. This implies that if we use a single model for the MITL annotations, the resulting dataset is highly unlikely to treat the methods differently. Second, the general bias measurements decrease with the number of involved models in the MITL annotation process. For the practical applications, hence, it is advisable to use multiple models to collect the label candidates to verify.

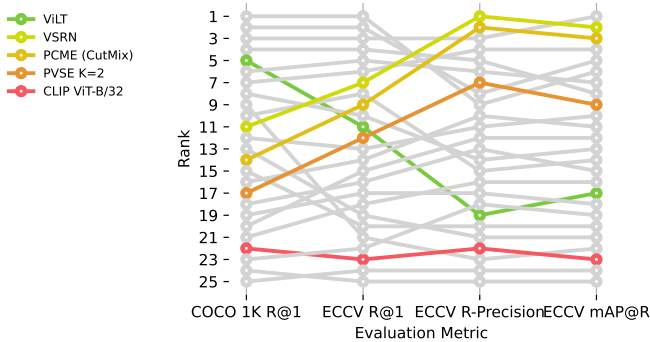
In practice, we observe that compared to COCO R@1, the rankings of the three models (PVSE, PCME and VSRN) improve and two models (CLIP, ViLT) are worsened in ECCV mAP@R (Figure E.3).



Figure E.1: **Overview of our machine-in-the-loop annotation process.** We choose the subset of the verified image caption pairs by crowd workers to control the effect by the models to final annotations.



Figure E.2: **Number of models vs. bias quantity.** The bias quantities (Eq. (E.5)) with changing the number of models for the annotation filtering process are shown. For both Recall@1 and R-Precision metrics, we observe that using more models reduce the severity of bias; the discrepancy between the resulting annotations by models and the underlying labels for the samples decreases.



(a) Rankings of selected models.

Figure E.3: **Bias quantity in the dataset.** (a) The bias quantities with changing the number of models for MITL are shown. We observe that using more models reduce the severity of bias; the discrepancy between the resulting annotations by models and the underlying labels for the samples decreases. (b) The full rankings of the chosen MITL annotators on our benchmark.

## References

- [1] Tsung-Yi Lin, Michael Maire, Serge Belongie, James Hays, Pietro Perona, Deva Ramanan, Piotr Dollár, and C Lawrence Zitnick. Microsoft coco: Common objects in context. In *Proc. ECCV*, 2014.
- [2] Xinlei Chen, Hao Fang, Tsung-Yi Lin, Ramakrishna Vedantam, Saurabh Gupta, Piotr Dollár, and C Lawrence Zitnick. Microsoft coco captions: Data collection and evaluation server. *arXiv preprint arXiv:1504.00325*, 2015.
- [3] Piyush Sharma, Nan Ding, Sebastian Goodman, and Radu Soricut. Conceptual captions: A cleaned, hypernymed, image alt-text dataset for automatic image captioning. In *ACL*, pages 2556–2565, 2018.
- [4] Soravit Changpinyo, Piyush Sharma, Nan Ding, and Radu Soricut. Conceptual 12m: Pushing web-scale image-text pre-training to recognize long-tail visual concepts. In *Proc. CVPR*, pages 3558–3568, 2021.
- [5] Karan Desai, Gaurav Kaul, Zubin Aysola, and Justin Johnson. RedCaps: Web-curated image-text data created by the people, for the people. In *NeurIPS Datasets and Benchmarks*, 2021.
- [6] Andrea Frome, Greg S Corrado, Jon Shlens, Samy Bengio, Jeff Dean, Marc’Aurelio Ranzato, and Tomas Mikolov. Devise: A deep visual-semantic embedding model. In *Proc. NeurIPS*, pages 2121–2129, 2013.
- [7] Peter Young, Alice Lai, Micah Hodosh, and Julia Hockenmaier. From image descriptions to visual denotations: New similarity metrics for semantic inference over event descriptions. *ACL*, 2:67–78, 2014.
- [8] Ryan Kiros, Ruslan Salakhutdinov, and Richard S Zemel. Unifying visual-semantic embeddings with multimodal neural language models. *arXiv preprint arXiv:1411.2539*, 2014.
- [9] Fartash Faghri, David J Fleet, Jamie Ryan Kiros, and Sanja Fidler. VSE++: Improving visual-semantic embeddings with hard negatives. In *Proc. BMVC*, 2018.
- [10] Jiuxiang Gu, Jianfei Cai, Shafiq R Joty, Li Niu, and Gang Wang. Look, imagine and match: Improving textual-visual cross-modal retrieval with generative models. In *Proceedings of the IEEE conference on computer vision and pattern recognition*, pages 7181–7189, 2018.
- [11] Kuang-Huei Lee, Xi Chen, Gang Hua, Houdong Hu, and Xiaodong He. Stacked cross attention for image-text matching. In *Proc. ECCV*, 2018.
- [12] Yan Huang, Qi Wu, Chunfeng Song, and Liang Wang. Learning semantic concepts and order for image and sentence matching. In *Proceedings of the IEEE Conference on Computer Vision and Pattern Recognition*, pages 6163–6171, 2018.

- [13] Kunpeng Li, Yulun Zhang, Kai Li, Yuanyuan Li, and Yun Fu. Visual semantic reasoning for image-text matching. In *Proc. ICCV*, pages 4654–4662, 2019.
- [14] Yale Song and Mohammad Soleymani. Polysemous visual-semantic embedding for cross-modal retrieval. In *Proc. CVPR*, pages 1979–1988, 2019.
- [15] Jonatas Wehrmann, Douglas M Souza, Mauricio A Lopes, and Rodrigo C Barros. Language-agnostic visual-semantic embeddings. In *Proceedings of the IEEE/CVF International Conference on Computer Vision*, pages 5804–5813, 2019.
- [16] Hao Wu, Jiayuan Mao, Yufeng Zhang, Yuning Jiang, Lei Li, Weiwei Sun, and Wei-Ying Ma. Unified visual-semantic embeddings: Bridging vision and language with structured meaning representations. In *Proceedings of the IEEE/CVF Conference on Computer Vision and Pattern Recognition*, pages 6609–6618, 2019.
- [17] Haoran Wang, Ying Zhang, Zhong Ji, Yanwei Pang, and Lin Ma. Consensus-aware visual-semantic embedding for image-text matching. In *Proc. ECCV*, 2020.
- [18] Tianlang Chen, Jiajun Deng, and Jiebo Luo. Adaptive offline quintuplet loss for image-text matching. In *Proc. ECCV*, 2020.
- [19] Haiwen Diao, Ying Zhang, Lin Ma, and Huchuan Lu. Similarity reasoning and filtration for image-text matching. In *Proc. AAAI*, 2021.
- [20] Sanghyuk Chun, Seong Joon Oh, Rafael Sampaio De Rezende, Yannis Kalantidis, and Diane Larlus. Probabilistic embeddings for cross-modal retrieval. In *Proc. CVPR*, 2021.
- [21] Jiacheng Chen, Hexiang Hu, Hao Wu, Yuning Jiang, and Changhu Wang. Learning the best pooling strategy for visual semantic embedding. In *Proc. CVPR*, 2021.
- [22] Zhenyu Huang, Guocheng Niu, Xiao Liu, Wenbiao Ding, Xinyan Xiao, hua wu, and Xi Peng. Learning with noisy correspondence for cross-modal matching. In A. Beygelzimer, Y. Dauphin, P. Liang, and J. Wortman Vaughan, editors, *Proc. NeurIPS*, 2021.
- [23] Ali Furkan Biten, Andres Mafla, Lluís Gómez, and Dimosthenis Karatzas. Is an image worth five sentences? a new look into semantics for image-text matching. In *Proceedings of the IEEE/CVF Winter Conference on Applications of Computer Vision*, pages 1391–1400, 2022.
- [24] Alec Radford, Jong Wook Kim, Chris Hallacy, Aditya Ramesh, Gabriel Goh, Sandhini Agarwal, Girish Sastry, Amanda Askell, Pamela Mishkin, Jack Clark, Gretchen Krueger, and Ilya Sutskever. Learning transferable visual models from natural language supervision. In Marina Meila and Tong Zhang, editors, *Proc. ICML*, volume 139 of *Proceedings of Machine Learning Research*, pages 8748–8763. PMLR, 18–24 Jul 2021.
- [25] Catherine Wah, Steve Branson, Peter Welinder, Pietro Perona, and Serge Belongie. The caltech-ucsd birds-200-2011 dataset, 2011.
- [26] Jonathan Krause, Michael Stark, Jia Deng, and Li Fei-Fei. 3d object representations for fine-grained categorization. In *Proc. CVPR Workshops*, pages 554–561, 2013.
- [27] Hyun Oh Song, Yu Xiang, Stefanie Jegelka, and Silvio Savarese. Deep metric learning via lifted structured feature embedding. In *Proc. CVPR*, pages 4004–4012, 2016.
- [28] Ziwei Liu, Ping Luo, Shi Qiu, Xiaogang Wang, and Xiaoou Tang. Deepfashion: Powering robust clothes recognition and retrieval with rich annotations. In *Proc. CVPR*, pages 1096–1104, 2016.
- [29] Kevin Musgrave, Serge Belongie, and Ser-Nam Lim. A metric learning reality check. In *Proc. ECCV*, 2020.
- [30] Wonjae Kim, Bokyung Son, and Ildoo Kim. Vilt: Vision-and-language transformer without convolution or region supervision. In *Proc. ICML*, 2021.
- [31] Zarana Parekh, Jason Baldridge, Daniel Cer, Austin Waters, and Yinfei Yang. Crisscrossed captions: Extended intramodal and intermodal semantic similarity judgments for ms-coco. *arXiv preprint arXiv:2004.15020*, 2020.

[32] Daniel Cer, Yinfei Yang, Sheng-yi Kong, Nan Hua, Nicole Limtiaco, Rhomni St John, Noah Constant, Mario Guajardo-Cespedes, Steve Yuan, Chris Tar, et al. Universal sentence encoder. In *Proc. EMNLP*, 2018.

[33] Jeffrey Pennington, Richard Socher, and Christopher D Manning. Glove: Global vectors for word representation. In *Proc. EMNLP*, pages 1532–1543, 2014.

[34] Rion Snow, Brendan O’Connor, Daniel Jurafsky, and Andrew Ng. Cheap and fast – but is it good? evaluating non-expert annotations for natural language tasks. In *Proceedings of the 2008 Conference on Empirical Methods in Natural Language Processing*, pages 254–263, Honolulu, Hawaii, October 2008. Association for Computational Linguistics.

[35] Alexander Sorokin and David Forsyth. Utility data annotation with amazon mechanical turk. In *2008 IEEE Computer Society Conference on Computer Vision and Pattern Recognition Workshops*, pages 1–8, 2008.

[36] Panagiotis G Ipeirotis, Foster Provost, and Jing Wang. Quality management on amazon mechanical turk. In *Proceedings of the ACM SIGKDD workshop on human computation*, pages 64–67, 2010.

[37] Ninareh Mehrabi, Fred Morstatter, Nripsuta Saxena, Kristina Lerman, and Aram Galstyan. A survey on bias and fairness in machine learning. *ACM Comput. Surv.*, 54(6), July 2021.

[38] Luca Scimeca, Seong Joon Oh, Sanghyuk Chun, Michael Poli, and Sangdoo Yun. Which shortcut cues will dnns choose? a study from the parameter-space perspective. In *International Conference on Learning Representations (ICLR)*, 2022.

[39] Yuri Y Boykov and M-P Jolly. Interactive graph cuts for optimal boundary & region segmentation of objects in nd images. In *Proc. ICCV*, volume 1, pages 105–112. IEEE, 2001.

[40] Burr Settles. Active learning literature survey, 2009.

[41] Ning Xu, Brian Price, Scott Cohen, Jimei Yang, and Thomas S Huang. Deep interactive object selection. In *Proc. CVPR*, pages 373–381, 2016.

[42] Rodrigo Benenson, Stefan Popov, and Vittorio Ferrari. Large-scale interactive object segmentation with human annotators. In *Proc. CVPR*, pages 11700–11709, 2019.

[43] Minsuk Chang, Léonore V Guillain, Hyeungshik Jung, Vivian M Hare, Juho Kim, and Maneesh Agrawala. Recipescape: An interactive tool for analyzing cooking instructions at scale. In *Proceedings of the 2018 CHI Conference on Human Factors in Computing Systems*, pages 1–12, 2018.

[44] Anhong Guo, X. Chen, Haoran Qi, Samuel White, Suman Ghosh, C. Asakawa, and Jeffrey P. Bigham. Vizlens: A robust and interactive screen reader for interfaces in the real world. *Proceedings of the 29th Annual Symposium on User Interface Software and Technology*, 2016.

[45] Besmira Nushi, Ece Kamar, and E. Horvitz. Towards accountable ai: Hybrid human-machine analyses for characterizing system failure. In *HCOMP*, 2018.

[46] Wen Wu and Jie Yang. Smartlabel: An object labeling tool using iterated harmonic energy minimization. In *Proceedings of the 14th ACM international conference on Multimedia*, pages 891–900, 2006.

[47] Yashaswi Verma and CV Jawahar. Image annotation by propagating labels from semantic neighbourhoods. *IJCV*, 121(1):126–148, 2017.

[48] Mykhaylo Andriluka, Jasper RR Uijlings, and Vittorio Ferrari. Fluid annotation: a human-machine collaboration interface for full image annotation. In *Proceedings of the 26th ACM international conference on Multimedia*, pages 1957–1966, 2018.

[49] Alina Kuznetsova, Hassan Rom, Neil Alldrin, Jasper Uijlings, Ivan Krasin, Jordi Pont-Tuset, Shahab Kamali, Stefan Popov, Matteo Malloci, Alexander Kolesnikov, et al. The open images dataset v4. *IJCV*, 128(7):1956–1981, 2020.

[50] Christian Szegedy, Vincent Vanhoucke, Sergey Ioffe, Jon Shlens, and Zbigniew Wojna. Rethinking the inception architecture for computer vision. In *Proceedings of the IEEE conference on computer vision and pattern recognition*, pages 2818–2826, 2016.

[51] Kaiming He, Xiangyu Zhang, Shaoqing Ren, and Jian Sun. Deep residual learning for image recognition. In *Proc. CVPR*, 2016.

[52] Toni Kaplan, S. Saito, Kotaro Hara, and Jeffrey P. Bigham. Striving to earn more: A survey of work strategies and tool use among crowd workers. In *HCOMP*, 2018.

[53] Jean Y. Song, Raymond Fok, Alan Lundgard, Fan Yang, Juho Kim, and Walter S. Lasecki. Two tools are better than one: Tool diversity as a means of improving aggregate crowd performance. *23rd International Conference on Intelligent User Interfaces*, 2018.

[54] John Joon Young Chung, Jean Y. Song, Sindhu Kutty, Sungsoo Hong, Juho Kim, and Walter S. Lasecki. Efficient elicitation approaches to estimate collective crowd answers. *Proceedings of the ACM on Human-Computer Interaction*, 3:1 – 25, 2019.

[55] Michael S Bernstein, Greg Little, Robert C Miller, Björn Hartmann, Mark S Ackerman, David R Karger, David Crowell, and Katrina Panovich. Soylent: a word processor with a crowd inside. In *Proceedings of the 23nd annual ACM symposium on User interface software and technology*, pages 313–322, 2010.

[56] Juho Kim, P. Nguyen, Sarah A. Weir, Philip J. Guo, Rob Miller, and Krzysztof Z Gajos. Crowd-sourcing step-by-step information extraction to enhance existing how-to videos. *Proceedings of the SIGCHI Conference on Human Factors in Computing Systems*, 2014.

[57] Kyunghyun Cho, Bart Van Merriënboer, Dzmitry Bahdanau, and Yoshua Bengio. On the properties of neural machine translation: Encoder-decoder approaches. *arXiv preprint arXiv:1409.1259*, 2014.

[58] Ashish Vaswani, Noam Shazeer, Niki Parmar, Jakob Uszkoreit, Llion Jones, Aidan N Gomez, Łukasz Kaiser, and Illia Polosukhin. Attention is all you need. In *Proc. NeurIPS*, pages 5998–6008, 2017.

[59] Shaoqing Ren, Kaiming He, Ross Girshick, and Jian Sun. Faster r-cnn: Towards real-time object detection with region proposal networks. In *Proc. NeurIPS*, pages 91–99, 2015.

[60] Alexey Dosovitskiy, Lucas Beyer, Alexander Kolesnikov, Dirk Weissenborn, Xiaohua Zhai, Thomas Unterthiner, Mostafa Dehghani, Matthias Minderer, Georg Heigold, Sylvain Gelly, Jakob Uszkoreit, and Neil Houlsby. An image is worth 16x16 words: Transformers for image recognition at scale. In *Proc. ICLR*, 2021.

[61] Sangdoo Yun, Dongyoon Han, Seong Joon Oh, Sanghyuk Chun, Junsuk Choe, and Youngjoon Yoo. Cutmix: Regularization strategy to train strong classifiers with localizable features. In *Proc. ICCV*, 2019.

[62] Maurice G Kendall. A new measure of rank correlation. *Biometrika*, 30(1/2):81–93, 1938.

[63] Andrej Karpathy and Li Fei-Fei. Deep visual-semantic alignments for generating image descriptions. In *Proc. CVPR*, pages 3128–3137, 2015.

[64] Peter Anderson, Xiaodong He, Chris Buehler, Damien Teney, Mark Johnson, Stephen Gould, and Lei Zhang. Bottom-up and top-down attention for image captioning and visual question answering. In *Proc. CVPR*, 2018.

[65] Pengchuan Zhang, Xiuju Li, Xiaowei Hu, Jianwei Yang, Lei Zhang, Lijuan Wang, Yejin Choi, and Jianfeng Gao. Vinvl: Making visual representations matter in vision-language models. In *Proc. CVPR*, 2021.

[66] Junnan Li, Dongxu Li, Caiming Xiong, and Steven Hoi. Blip: Bootstrapping language-image pre-training for unified vision-language understanding and generation, 2022.

[67] Florian Schroff, Dmitry Kalenichenko, and James Philbin. Facenet: A unified embedding for face recognition and clustering. In *Proc. CVPR*, pages 815–823, 2015.

[68] Ranjay Krishna, Yuke Zhu, Oliver Groth, Justin Johnson, Kenji Hata, Joshua Kravitz, Stephanie Chen, Yannis Kalantidis, Li-Jia Li, David A Shamma, et al. Visual genome: Connecting language and vision using crowdsourced dense image annotations. *IJCV*, 123(1):32–73, 2017.

[69] Dhruv Kumar Mahajan, Ross B. Girshick, Vignesh Ramanathan, Kaiming He, Manohar Paluri, Yixuan Li, Ashwin Bharambe, and Laurens van der Maaten. Exploring the limits of weakly supervised pretraining. In *Proc. ECCV*, 2018.

[70] Byeongho Heo, Sanghyuk Chun, Seong Joon Oh, Dongyoon Han, Sangdoo Yun, Gyuwan Kim, Youngjung Uh, and Jung-Woo Ha. Adamp: Slowing down the slowdown for momentum optimizers on scale-invariant weights. In *Proc. ICLR*, 2021.

[71] Ilya Loshchilov and Frank Hutter. Sgdr: Stochastic gradient descent with warm restarts. In *Proc. ICLR*, 2017.

[72] Jacob Devlin, Ming-Wei Chang, Kenton Lee, and Kristina Toutanova. BERT: pre-training of deep bidirectional transformers for language understanding. In Jill Burstein, Christy Doran, and Thamar Solorio, editors, *Proceedings of the 2019 Conference of the North American Chapter of the Association for Computational Linguistics: Human Language Technologies, NAACL-HLT 2019, Minneapolis, MN, USA, June 2-7, 2019, Volume 1 (Long and Short Papers)*, pages 4171–4186. Association for Computational Linguistics, 2019.

[73] Robert Geirhos, Carlos RM Temme, Jonas Rauber, Heiko H Schütt, Matthias Bethge, and Felix A Wichmann. Generalisation in humans and deep neural networks. In *Advances in Neural Information Processing Systems*, pages 7538–7550, 2018.

[74] Olga Russakovsky, Jia Deng, Hao Su, Jonathan Krause, Sanjeev Satheesh, Sean Ma, Zhiheng Huang, Andrej Karpathy, Aditya Khosla, Michael Bernstein, et al. Imagenet large scale visual recognition challenge. *International journal of computer vision*, 115(3):211–252, 2015.

[75] Dhruv Mahajan, Ross Girshick, Vignesh Ramanathan, Kaiming He, Manohar Paluri, Yixuan Li, Ashwin Bharambe, and Laurens Van Der Maaten. Exploring the limits of weakly supervised pretraining. In *Proc. ECCV*, pages 181–196, 2018.

[76] Mannat Singh, Laura Gustafson, Aaron Adcock, Vinicius de Freitas Reis, Bugra Gedik, Raj Prateek Kosaraju, Dhruv Mahajan, Ross Girshick, Piotr Dollár, and Laurens van der Maaten. Revisiting weakly supervised pre-training of visual perception models, 2022.

[77] Chao Jia, Yinfei Yang, Ye Xia, Yi-Ting Chen, Zarana Parekh, Hieu Pham, Quoc Le, Yun-Hsuan Sung, Zhen Li, and Tom Duerig. Scaling up visual and vision-language representation learning with noisy text supervision. In *Proc. ICML*, pages 4904–4916. PMLR, 2021.

[78] Sangdoo Yun, Seong Joon Oh, Byeongho Heo, Dongyoon Han, Junsuk Choe, and Sanghyuk Chun. Re-labeling imagenet: from single to multi-labels, from global to localized labels. In *Proc. CVPR*, 2021.

[79] Hongyi Zhang, Moustapha Cisse, Yann N Dauphin, and David Lopez-Paz. mixup: Beyond empirical risk minimization. In *Proc. ICLR*, 2018.

[80] Ekin D Cubuk, Barret Zoph, Dandelion Mane, Vijay Vasudevan, and Quoc V Le. Autoaugment: Learning augmentation strategies from data. In *Proc. CVPR*, pages 113–123, 2019.

[81] Ekin D Cubuk, Barret Zoph, Jonathon Shlens, and Quoc V Le. Randaugment: Practical automated data augmentation with a reduced search space. In *Proc. CVPR Workshops*, pages 702–703, 2020.

[82] Maxime Kayser, Oana-Maria Camburu, Leonard Salewski, Cornelius Emde, Virginie Do, Zeynep Akata, and Thomas Lukasiewicz. e-vil: A dataset and benchmark for natural language explanations in vision-language tasks, 2021.

[83] Christoph Sager, Christian Janiesch, and Patrick Zschech. A survey of image labelling for computer vision applications. *Journal of Business Analytics*, pages 1–20, 2021.

[84] Richard A Johnson, Irwin Miller, and John E Freund. *Probability and statistics for engineers*, volume 2000. Pearson Education London, 2000.

- [85] Christopher M Bishop. Pattern recognition. *Machine learning*, 128(9), 2006.
- [86] Scott Plous. *The psychology of judgment and decision making*. McGraw-Hill Book Company, 1993.
- [87] Phillipa J Easterbrook, Ramana Gopalan, JA Berlin, and David R Matthews. Publication bias in clinical research. *The Lancet*, 337(8746):867–872, 1991.
- [88] Marc Mangel and Francisco J Samaniego. Abraham wald’s work on aircraft survivability. *Journal of the American Statistical Association*, 79(386):259–267, 1984.